Anonymous Referee #1

Review of "Open fires in Greenland: an unusual event and its impact on the albedo of the Greenland Ice Sheet" by N. Evangeliou and co-authors.
General comments.

N. Evangeliou and co-authors present a paper dealing with the atmospheric emission of black carbon by peat fires in Greenland during an extreme event in August 2017. They estimate the total amount of BC released in the atmosphere and its impact on the atmospheric radiative balance and snow albedo. The authors conclude that none of those impact are really significant. I found the paper lacking a focused scientific objective and finally it will have a limited interest for the scientific community. The methodology is sound but many of the assumptions must be clarify. The validation exercise is too qualitative while the dataset can be used for quantitative assessment. The conclusion that peat fire in Greenland could be of a significant importance for climate is not really supported by the findings of this paper.

Response: We agree that the methodology and parts of the discussion needed lots of improvement and we have made substantial effort with numerous changes in all parts of the manuscript according to both reviewers' suggestions (please see manuscript with Track Changes).

However, we do not agree with this description of our work. The validation is qualitative because no direct measurements of BC concentrations exist from this event occurring in a particularly data-sparse region, and also few satellite data document the event. The only data we found are Lidar data from CALIPSO that confirmed the presence of the plume where our model predicted it. Could the reviewer suggest, in concrete terms, which dataset could be used for quantitative assessment?

The reviewer says, "The conclusion that peat fire in Greenland could be of a significant importance for climate is not really supported by the findings of this paper." This is NOT a conclusion, but a logical probability, considering that 25% of Greenland's surface is permafrost that is rich in peat. We now show this more clearly in the updated version of our manuscript. In addition, NASA's satellites show an increasing trend of fires in thawed permafrost over Greenland (**see new supplementary figure S1 or attached Fig. R1**) and our simulations showed that 30% of the emissions were deposited in the Greenland Ice Sheet (**Lines 388-391**).

We disagree with the comment of the reviewer that this paper will have a limited interest for the scientific community. We present some statistics from the ACP Discussions website.
In the Discussions page of the journal (https://www.atmos-chem-phys-discuss.net/discussion_papers.html), at the time that we started writing this response (22-05-2018), there are 30 papers in open discussion (ACPD) that were published the same time as ours (March 2018). If we calculate the average views and downloads we get **302±100 (min: 199 – max: 570)**, while our paper's visibility is **293**.

Furthermore, although media coverage does not converge with scientific quality, the present study was selected for a press conference on "Shape of things to come? The 2017 wildfire season" during the EGU 2018 conference (https://client.cntv.at/egu2018/pc5).

Specific comments.
Abstract
Line 43. Your conclusion doesn't support this fact and it's not scientifically based.
Response: Line 43 states "If the expected further warming of Greenland produces much larger fires in the future, this could indeed cause substantial albedo changes and thus lead to accelerated melting of the Greenland Ice Sheet." This sentence is NOT a conclusion, but a logical hypothesis (if). We have slightly rephrased the sentence, so it now reads: "If the expected future warming of the Arctic produces more fires in Greenland, this could indeed cause albedo changes and thus contribute to accelerated melting of the Greenland Ice Sheet." Finally, in order to prove that this is not pure speculation but a solid hypothesis, we support it with references (see last paragraph in conclusions).

Introduction.
The introduction is missing a comprehensive literature review on Arctic peat ecosystem and fire occurrence to better understand why those particular fires have been studied.
Response: We have focused our introduction on peatlands and fires in Greenland and think that a more comprehensive literature review on Arctic peat ecosystems in general is out of scope of this paper. After all, this paper studies the impact of fires in Greenland on BC concentration and deposition in Greenland, not on future scenarios of fire occurrence, permafrost melt or such.

Line 83-84. Provide evidence of the significance of this event compared to other events.
Response: Our statement that "… the fires … , probably represent the largest fires that have occurred on Greenland in modern times.", is now supported by a new plot of the number of MODIS active fire detections (MODIS MCD14DL) over Greenland (**see new supplementary Figure S1 or attached Fig.R1**).

Method
L89-118. This section is very important as it is the starting point for the estimation of the BC amount released by fires. However the methodology used (eg. which sensor, when, spatial resolution, who and how has done the estimation, . . .) is unclear. On Line 241, we can read that the burnt surface area comes from GlobeCover 2009. So finally, what is your point?
Response: Line 241 has been corrected. We appreciate the reviewer for this constructive comment.
As regards to the methodology, we have done a few corrections to explain better what has been done, also giving specifications of the products we used (lines 97-99).
In our opinion, detailed explanations on the calculations are not needed, since the method has been already published in the relevant literature and used in many other previous cases. As we explain in the manuscript, the burned area was mapped using severity levels of dNBR index. The methodology of its application is described in details in Lutes et al. (2006) (pp. 201-270), which is **attached**. There is another paper describing how dNBR was calibrated in field - Escuin et all, 2008 (see reference in the manuscript). Since the index is sensitive to any disturbances, we applied a manually delineated fire perimeter to increase the accuracy of mapping.

You should rewrite this section with a detailed comment of Table 1 and explain how it compares to active fire mapping. Line 118 needs clarification based on quantitative information.

<u>Response</u>: Line 94 explicitly says that the location of the active fires were downloaded from NASA's website. So, what is shown in Table 1 has been confirmed with NASA's active fires (also shown in supplements' Figure S1 and attached Fig.R1).

Regarding to the severity levels (Line 118), qualitative information is given in Key and Benson (2006) together with all the details of the methodology used. The same methodology has been used to map the Chernobyl fires (see: Evangeliou et al., 2014; 2015; 2016)

The comment to confirm Line 118 based on quantitative information is too generic and we do not really understand what the reviewer wants us to do.

L155 Explain how you get this number and provide a range of possible values

<u>Response</u>: Line 155 says "In contrast, tropical peatlands can have deep burn depths of 40–50 cm and release an average of 300–450 t C ha^{-1} (Page et al., 2015; Reddy et al., 2015)."

It should be obvious that this range of values was reported by Page et al. (2015) and Reddy et al. (2015).

If the reviewer means the average amount of organic fuel available for combustion that we used for the Greenland fires (100 t C ha^{-1}), it has been taken from Smirnov et al. (2015). In this paper, it was assumed that for peat-bog fires, the average amount of fuel available for combustion (including the soil organic matter) is up to 120 t/ha supported from measurements from IPCC (2006).

L180. Provide reference for BC density and size distribution. Peat fires emits large amount of organic carbon. The possible impact of the mixing state of BC and POM on aerosol size distribution, optical properties and residence time should be discuss in this paper.

<u>Response</u>: We agree that fires also emit large quantities of organic carbon (OC). However, the impact of OC on the albedo of the ice sheet is probably small, although it probably enhances the BC effect, since OC can also be slightly absorbing (e.g., brown carbon). But given the lack of information on the optical properties of the emitted OC, we think an additional analysis of OC would not be very meaningful.

With respect to BC density and size distribution, a reference was added in Line 214 of the updated manuscript. We have now also performed a sensitivity study on the impact of different particle size distributions on the deposition of BC over Greenland's Ice Sheet and discuss it in section 3.2. A detailed analysis of residence times of BC has been already presented by Grythe et al. (2017) [reference in the manuscript] and in Evangeliou et al. (2018) [reference under editorial check in ACP Discussions].

L200 and discussion section 3.3
The apportionment between emission from peat fires and other sources remains un-clear for me. The methodology is not same as the one use for assessing impact of peat fire. The figure 4 is not really useful while other figures are in the supplement material.

<u>Response</u>: Lagrangian models such as the one used in our work (FLEXPARTv10) can run forward in time (like CTMs or climate models) using specific emissions that can be taken from an existing inventory (for example ECLIPSE, see:

).
Moreover, Lagrangian models have the advantage that they can also run backward in time, from a specific point or region for which the user wants to calculate concentrations. What is produced then is the footprint emission sensitivity (or footprint), which is simply the residence time of the computational particles (in sec) in each grid-cell of the model. Then, by multiplying this footprint with a given emission inventory (e.g. ECLIPSE) given in $kg/m^2/s$ and dividing with the altitude of the lowest vertical level in the model, one obtains surface concentrations again. Notice that forward and backward calculations are equivalent, so the methodology is not different. However, depending on the setup, the computational efficiency can be much higher in backward mode, and that is also the reason we used it to assess the impact of emissions outside Greenland.

For FLEXPART that we used in this study, a comparison between forward and backward simulations can be found in Seibert and Frank (2004).

We calculate average concentrations of surface BC in four compartments of Greenland based on ECLIPSE emissions. ECLIPSE includes all anthropogenic sources, while we calculate biomass burning emissions using global MODIS-satellite hot spot data (Giglio et al., 2016) and GFAS (references in the manuscript). Everything is well documented in the associated references.

Figure 4 has been replaced by Figure S4 as suggested.

L204 and section 4.2
The methodology and the discussion section on RF computation must be improved and clearly states how you deal with both surface albedo and atmospheric effect of BC on the radiative balance. Figure 7 is confusing as it deals with both BOA, TOA, time series and geographical distribution as the same time.
Response: We have re-written and re-structured the whole chapter, both in the Methodology and analysis of the Results (see manuscript with Truck Changes). Our perception is not to present in detail methods that have been documented in previous publications. For RF calculations we used the uvspec model from the libRadtran radiative transfer software package (http://www.libradtran.org/doku.php) (see references in the manuscript: Emde et al., 2016; Mayer and Kylling, 2005). Snow albedo was calculated with the SNICAR model (http://snow.engin.umich.edu/info.html) in a two-layer configuration (see references in the manuscript: Flanner et al., 2007, 2009). These are open source codes that have been used by many groups worldwide.
Figure 7 has been improved as suggested.

L218 and section 4.1 along with Figures 5 and 6. The validation exercise is really too qualitative and based on visual inspection of satellite data that are not really used scientifically. AERONET data can provide detailed information on aerosol optical properties and radiative forcing. CALIOP data products give aerosol extinction profiles which can be used in the RF computations.
Response: The reason the validation exercise is so qualitative is that we have no clear observations of the Greenland fire plume. The AERONET data show impacts of the forest fires burning outside Greenland. Only at one site, the AERONET data show an AOD increase that is partly (but not exclusively) due to the Greenland fires.

L466 Your last bullet point is rather speculative and not supported by the findings of the paper.
Response: This is true and we have now corrected it. The last bullet is NOT ALL OF IT a conclusion, but rather a comment and therefore, we now show it as a comment (not bulleted) below the bullet. We further support what we say in the sentence with references.

REFERENCES

Lutes, Duncan C.; Keane, Robert E.; Caratti, John F.; Key, Carl H.; Benson, Nathan C.; Sutherland, Steve; Gangi, Larry J. 2006. FIREMON: Fire effects monitoring and inventory system. Gen. Tech. Rep. RMRS-GTR-164-CD. Fort Collins, CO: U.S. Department of Agriculture, Forest Service, Rocky Mountain Research Station. (ATTACHED)

Key, C. H. and Benson, N. C.: Landscape assessment: Sampling and analysis methods, USDA For. Serv. Gen. Tech. Rep. RMRS-GTR-164-CD, (June), 1–55, doi:10.1002/app.1994.070541203, 2006.

Evangeliou, N., Balkanski, Y., Cozic, A., Hao, W. M. and Møller, A. P.: Wildfires in Chernobyl-contaminated forests and risks to the population and the environment: A new nuclear disaster about to happen?, Environ. Int., 73, 346–358, doi:10.1016/j.envint.2014.08.012, 2014.

Evangeliou, N., Balkanski, Y., Cozic, A., Hao, W. M., Mouillot, F., Thonicke, K., Paugam, R., Zibtsev, S., Mousseau, T. A., Wang, R., Poulter, B., Petkov, A., Yue, C., Cadule, P., Koffi, B., Kaiser, J. W., Møller, A. P. and Classen, A. T.: Fire evolution in the radioactive forests of Ukraine and Belarus: Future risks for the population and the environment, Ecol. Monogr., 85(1), 49–72, doi:10.1890/14-1227.1, 2015.

Evangeliou, N., Zibtsev, S., Myroniuk, V., Zhurba, M., Hamburger, T., Stohl, A., Balkanski, Y., Paugam, R., Mousseau, T. A., Møller, A. P. and Kireev, S. I.: Resuspension and atmospheric transport of radionuclides due to wildfires near the Chernobyl Nuclear Power Plant in 2015: An impact assessment., Sci. Rep., 6, 26062 [online] Available from: http://www.nature.com/srep/2016/160517/srep26062/full/srep26062.html, 2016.

Smirnov, N. S., Korotkov, V. N. and Romanovskaya, A. A.: Black carbon emissions from wildfires on forest lands of the Russian Federation in 2007–2012, Russ. Meteorol. Hydrol., 40(7), 435–442, doi:10.3103/S1068373915070018, 2015

2006 IPCC Guidelines for National Greenhouse Gas Inventories, Vol. 4: Agriculture, Forestry and Other Land Use (IPCC, 2006) [in Russian].

Seibert, P. and Frank, A.: Source-receptor matrix calculation with a Lagrangian particle dispersion model in backward mode, Atmos. Chem. Phys., 4(1), 51–63, doi:10.5194/acp-4-51-2004, 2004.

Giglio, L., Descloitres, J., Justice, C. O. and Kaufman, Y. J.: An enhanced contextual fire detection algorithm for MODIS, Remote Sens. Environ., 87(2–3), 273–282, doi:10.1016/S0034-4257(03)00184-6, 2003.

Anonymous Referee #2

General comments :
This work investigates the quantification of emissions of black carbon (BC) from intense fires on peat lands in Western Greenland during summer 2017 and their impacts on albedo reduction and radiative forcing. The authors conclude that those impacts of BC deposition of the Greenland Ice Sheet are almost negligible, which turns out to be a scientific result for the community. This study is interesting and sound for ACP. I have nevertheless several criticisms requiring a careful and revision and in-depth improvements both in the methodology, often unclear, and in the discussion of the results before the paper is suitable for publication in ACP.
Response: We acknowledge the reviewer's comments and his effort to improve this manuscript. We have tried to follow his suggestions to correct the manuscript and have basically re-written parts of the manuscript (please see manuscript with Track Changes).

 Specific comments :
L1-2 : The title seems to indicate that the main focus of the paper is the quantification of the reduction in albedo due to open fires in Greenland. Only ten lines in the paper really focus on the modification of the albedo due to BC deposition. The title should reflect the main findings of the paper : quantification of BC emissions of this unusual event, transport of the plume, deposition.
Response: We agree; we have changed the title to "Open fires in Greenland in summer 2017: transport and deposition of BC and impact on the Greenland Ice Sheet"

L41-44 and L496-500 : I find a bit strange to conclude both abstract and conclusion by something purely speculative and that does not match the main results of the paper.
Response: We admit that this is probably an extreme formulation and we have changed it to a weaker statement. We would like to draw attention that this statement is not a conclusion, but a logical hypothesis. To further show that it's not a conclusion, we now support the paragraph with references (see last paragraph in conclusions).

L83-84 : "the largest fires". Give maybe statistics or cite a climatological study to support this assertion.
Response: We have plotted the annual number of active fires from NASA's MODIS product in supplements' Figure S1 (or Fig.R1) starting from first year that satellite data were available (2001).

L111 : The authors should give more details about the procedure applied on the data. "Additional classification" is too vague.
Response: The statement has been removed!

L130 : "assuming a 6h persistence". How is this hypothesis justified ? Is it confirmed b observations or by other studies ?
Response: Well, this is confirmed by previous studies (Kaiser et al., 2012 – reference in the paper). We chose a persistence model similar to what is done in Kaiser et al. (2012) and used a time of the same order of magnitude with the mean return time of MODIS in the afternoon (peak time of fire) ~ 4h. For a description of the persistence model that was used, please see line 8 - page 9852 of Paugam et al. (2015).

L161 : Say clearly that the only variable computed in this study from measurements is the burned area A. The other factors are based on assumptions or provided by previous studies.
Response: Corrected. This is now explicitly mentioned in Line 184.

L181 : Those values suggest that aerosols are not only composed of BC (which is a reasonable assumption). How do the authors justify this size distribution ? It has indeed a huge influence on the deposition efficiencies (both sedimentation and wet removal) and on the calculation of aerosol optical properties. Both the radiative forcings and reduction of albedo on snow surfaces will be sensitive to this assumption on the size distribution. I suggest that the authors perform a sensitivity study on the influence of those parameters.
Response: After rapid coagulation, more than 90% of the mass of BC after fires is present in sizes between 0.1 – 1 µm in the atmosphere. This has been highlighted by many experiments/measurements and is now well justified in section 3.2.

However, we have followed the suggestion of the current reviewer and performed a sensitivity study using different size distribution of the BC particles produced from the 2017 fires in Greenland and we calculated the uncertainty on the deposited mass of BC due to different size distribution. We present and discuss the results at the end of section 3.2. The effect of different size distribution on residence times has been already studied by Grythe et al. (2017) [reference in the manuscript] and the different deposition coefficients in Evangeliou et al. (2018) [reference under editorial check in ACP Discussions].
The calculated uncertainty from this sensitivity test ranges from 10%–30% in 86% of the Sheet's surface to up to 50% in the rest of the Sheet's surface.

L200 : "a simple emission scheme". What does it mean? Why don't the authors use the same methodology for all fires ?
Response: We appreciate reviewer's comment here. This was a typo error and we have updated this part of the methodology.

L200-201 : Those emission factors should depend on the type of soil and vegetation. Which maps have been used here ? Which values for emission factors have been finally chosen ? The reader should be able to reproduce the results of this study ; without such assumptions, it is impossible.
Response: Corrected; See previous comment.

Sect. 2.4 : Do the authors calculate radiative forcing assuming refractive index of BC only? The choice of the refractive index should be done in accordance with the size distribution (L181), which probably reflects an internal mixture of aerosols.
Response: The radiative forcing was calculated using the refractive index of BC only. We agree with the reviewer that BC was likely present as an internal mixture with other aerosol components (especially OC). However, we did not simulate OC and therefore used only the refractive index of BC. This will lead to an underestimation of the atmospheric effects of BC, since internal mixing with OC will likely enhance the BC absorption, and there may also be other absorbing components in the aerosol. However, we think that as an order of magnitude estimation of the atmospheric effects, our

assumption should be sufficient. Furthermore, the more important impact of BC on the albedo is less (or not) sensitive to the mixing state of the aerosols.

L226 : "we display" : where ?
Response: We substituted 'display' with 'used'.

L292 : "a small portion of the emitted BC". Please quantify it.
Response: We have quantified the portion that lifted up in this particular day (≈516 kg).

L334 : "due to the generally dry weather when the fires were burning". It can be also ascribed to the fact that dry deposition mostly occurs in the quasi-laminar sublayer close to the surface. Aerosols are quickly deposited close to the sources before being injected at higher altitudes and being transported away from sources.
Response: Thanks for this comment. We have included it in the manuscript.

L365 : "the anthropogenic contribution is larger". For the sake of clarity, the authors might write that the anthropogenic is relatively larger in Southern Greenland in contrast to Northern Greenland but remains lower than the biomass burning contribution.
Response: Comment was added to the manuscript.

L367 : "the BC concentrations that are calculated here for the studied fire period are relatively high compared to those reported previously". I am not sure this is always true. The authors should also quote more recent studies, e.g. Polashenski et al. (2015), Legrand et al. (2016) or Thomas et al. (2017), who have reported higher events of biomass burning BC deposition over Greenland. If the BC deposited on snow/ice surfaces is much larger in those studies, it also suggests higher surface BC concentrations.
Response: We thank the reviewer for providing the references and have added them to the previous section. Please see Line 425-426 for Polashenski et al (2015) and Legrand et al. papers.
However, the Thomas et al. paper is using another unit (g/m2) and without knowing the density of the samples no conversion to ng/g (units used in the present) can be applied.

L378 and L389 : "dosages". Do you mean concentrations / mixing ratios ?
Response: They are dosages of concentrations. It is now explained in the last paragraph of section 3.3 and in the caption of the respective Figure.

L397-398 : BC particles are probably not the main contributors to AOD in this region for two reasons : the BC loadings are rather low in comparison to other aerosol compounds and the diameter of BC-containing particles is much smaller than the wave- length (0.5 um). A better proxy of the temporal evolution of the integrated BC would be the absorbing AOD (AAOD), which is also often provided at AERONET stations. The AAOD/AOD would be also a good indicator of the contribution of BC to the total AOD (even if BC is not the only absorbing component). This should be shown on Fig. 5.
Response: The reviewer has a very good point here and we tried to retrieve AAOD data as he suggested.
Though in Kangerlussuaq and Thule no AAOD Level 2 data are available for July-September 2017, while in Narsarsuaq AAOD Level 2 data are available for 2 September 2017 (when the fires had been already extinguished).

In Andrews et al. (2017) paper is stated that "One obvious limitation of the AERONET inversion retrievals is that the uncertainty of the derived SSA becomes very large at low values of AOD (Dubovik et al., 2000). To minimize the effects of this uncertainty, the AERONET Level 2 data invalidate all absorption-related values if the AOD at wavelength 440 nm (AOD440) is below 0.4 (Dubovik et al., 2000, 2002; Holben et al., 2006)." In page 6043 of the same paper it is stated that "It should be noted that AERONET does not recommend the use of absorption-related parameters (e.g., SSA, AAOD and complex index of refraction) at AOD440 below 0.4." In our case, except for the characteristic peak of AOD that is attributed to the N. American fires, all the other AOD values were below 0.4.

Sometimes researchers use AAOD LEV 1.5 data, but these get high uncertainty (see Andrews et al, 2017). In page 6051 of the Andrews et al. (2017) paper is also stated that "Using the sum-of-squares propagation of errors to calculate the uncertainty in AAOD for both high and low AAOD cases results in an AAOD uncertainty of approximately 0.015 for both high- and low-AOD cases ... An AAOD uncertainty value of 0.015 suggests an uncertainty of about 60% in AAOD for AOD440 D0.5 and more than 140% uncertainty in AAOD for AOD440 < 0.2."

Therefore, we do not think that these uncertain LEV1.5 AAOD measurements should be plotted instead of AOD here. However, if the reviewer or the editor disagree, we have retrieved them and we could use them in a next step. Besides, we only used AOD as an indicator for the presence of the plume, and for that purpose it should be sufficient.

L401-407 : How do the authors explain the significant AOD enhancement at the beginning of September observed at Narsarsuaq station ?
Response: As the reviewer can see, in the attached **Fig.R2** we present the biomass burning BC from GFAS (upper panel) in the beginning of September and the footprint emission sensitivity from the Narsarsuaq station (bottom panel) on September 3rd. We observe that the highest footprint emission sensitivity is located exactly at the place where GFAS emissions are the highest (Canada). Therefore, we have a clear indication that the increase that the reviewer mentioned is due to the Canadian wildfires.

L422 : "was not studied". Does it mean that the transport of those North American fire plumes was not correctly captured by FLEXPART ? It is indeed impossible to see on Fig. 6d as the vertical scale is not appropriate.
Response: Here, we wanted to state that the existence of the N. American fires in the attenuated backscatter measurements that we get from CALIOP was not further studied. The study of the N. American fires is beyond the scope of this paper. We have used a better formulation in the manuscript now.

Sect. 4.2 : The authors should remind that they calculated only the forcing due to the Greenland fires, which is itself small compared to the North American or Eurasian fires. It should also be said explicitly that the calculated radiative forcing values does not include semi-direct nor indirect effects, which may be dominant here.
Response: We have rewritten the first part of the section to include the information requested by the referee.

L436 : "cloudless conditions". I do not understand the purpose of this. It is only an ideal simulation, which is not commented in the paper afterwards. What does it bring to the discussion ?

Response: The IRF for cloudless conditions is compared against IRF including clouds in the subsequent lines. IRF for cloudless conditions was included, as they show the potential maximum effect of the forcing. The results presented show that the clouds reduce both the TOA and BOA IRF.

L440-442 : It is not clear if the given values refer to the total radiative forcing of BC. What are the relative contributions of the direct radiative forcing of BC and of the radiative forcing of BC deposited on snow surfaces ? The authors also give the values without any uncertainty, but a lot of assumptions have been done to retrieve the BC emissions, the BC size distribution, the BC optical properties. Each of those hypothe- sis would lead to a range of values of IRF.

Response: The given values refer to the total instantaneous radiative forcing, that is including both the effect of atmospheric BC and BC deposited on the snow. The latter dominates the IRF contributing between 85 to 99 % depending on BC amount. This has been clarified in the manuscript.

The composition of the BC from the fire is not known. Hence average BC optical properties were adopted. We have subsequently performed an uncertainty analysis using realistic variations in BC optical properties. This uncertainty analysis is included in the supplementary material and referred to in the manuscript.

We have also performed a sensitivity study and estimated the uncertainty of the BC deposition over Greenland due to the use of different size distribution of BC particles (see answer to previous comments).

L 442: "Fig 7c depicts the temporal behaviour..." Does it represent calculations in cloudy conditions ?

Response: It is the cloudy conditions that are shown. This information has been added both in the text and the figure caption. The temporal behaviour is shown in Fig 7d. This typo has been corrected as well.

L443-444 : I don't see how this information (blue line) can be useful. The location of the pixel where the maximum IRF is found likely varies with time. Besides the analysis of this figure is not done in text. I recommend to remove it.

Response: We have removed the blue line from the plot. The idea of plotting the TOA max IRF was to show that the single pixel maximum and area averaged RFs peak at different times. However, we agree with the reviewer that this information was perhaps not so useful.

L448-455 : If the authors want to be able to compare their results to global studies, as it is done here, they need to multiply the value of RF by the area of the simulation domain to obtain a forcing value in watts, and then divide it by the surface area of the Earth to obtain an equivalent global radiative effect in mW/m2 that could be compared to results for global studies.

Response: The cited value from Skeie et al. (2011) is not a global value, but a value representative for the Greenland ice sheet (Fig 17 of Skeie et al., 2011). It is this value we are comparing against. The values from Myhre et al (2013) are included in order to give the reader a global value to compare against. This has been clarified in the text. It is clear that, on a global scale, the obtained RF values are negligible.

L453-455 : What about the impact of North American and Eurasian fires, whose plumes reach Greenland during the studied period ?

Response: These plumes are not the focus of the present study. Similar plumes have been studied before, so we don't think focusing on these plumes would provide a lot of new information beyond what has been published before. More technically, we only estimate the impact of these plumes using backward calculations, whereas RF calculations would require forward calculations. We think this is out of scope of the present paper.

What we have done, instead, is to calculate the impact of the N. American fires in the surface concentrations of BC over Greenland (see section 3.3). This proved that the BC concentrations from the N. American fires in August 2017 are more than 1 order of magnitude higher compared with those produced from the Greenland fires of August 2017 (see updated Figure 4).

L456-457 : What is the albedo reduction due to BC deposition that can be ascribed to Greenland fires / to fires outside Greenland / to anthropogenic sources ? If the goal of the paper is indeed to focus on the impact of the Greenland fires, quantifying this effect and comparing it to the relative contribution of the different sources would be really valuable for the paper. The authors should also compare their albedo reduction values to previous studies, e.g. Polashenski et al. (2015).

Response: We now compare our results to those of Polashenski et al. (2015) in section 4.2. The detailed study of the fires outside Greenland and from anthropogenic sources is beyond the scope of this paper. Notice that the albedo effects can't be done on the basis of the backward calculations done for the other sources and would require totally new forward simulations. However, giving the range of surface BC concentrations over Greenland (section 3.3 and Figure 4) is already enough to conclude that the event that we studied in the current paper has minor effects on the albedo or RF compared to BC from the N. American fires or from anthropogenic sources simply because of the different magnitude and duration of these fires.

Sect. 5 : The conclusions may be more quantitative.
For example : L478-479 : the ratio of BC deposition from the different sources can be given

Response: We have not quantified how big the deposition from anthropogenic and biomass burning sources is, and we have removed this sentence from the manuscript.

L481-483 : the AOD enhancement can be precised
Response: Corrected.

L488 : "albedo change due to the BC deposition". Which sources have been considered ?
Response: Corrected. It is the albedo change due to BC deposition from the Greenland fire of 2017.

L496-500 : Remove this purely speculative sentence. The opposite could also be said, given the findings of the paper.
Response: These lines state that "The very large fraction of the BC emissions deposited on the Greenland Ice Sheet (30% of the emissions) makes these fires very efficient climate forcers on a per unit emission basis. If the expected future warming of the Arctic (IPCC, 2013) produces more fires in Greenland in the future (Keegan et al., 2014), this

could indeed cause substantial albedo changes and thus contribute to accelerated melting of the Greenland Ice Sheet."
We do not understand why this is speculative. A fraction of 30% deposition on the Greenland ice sheet is substantial, much higher than from any other source type and source region, so – on a per unit mass basis – the forcing due to albedo change is efficient, even if it is small overall. The second sentence can perhaps be considered somewhat speculative, but we have now reformulated it and, moreover, we support it with references. Furthermore, it is not presented as a conclusion, so it should be very clear to the reader to what extent this sentence is speculative. We nevertheless consider it important enough to keep it.

The choice of the figures kept in the manuscript is rather strange. Most useful figures relevant for the discussion have been displaced to the Supplementary Material. I recommend to move them to the main paper.
Response: We have moved the figure with the calculated dosages to the manuscript (Fig. 4), as the dosages are discussed more in the text. We have now placed back to the supplements (Fig. S5) the figure of the footprint emission sensitivities that are not the main focus of the paper. We are willing to put more figures in the manuscript in a next step, if the reviewer point into this direction. The only reason for using limited number of figures was that this paper was intended to be short.

Fig. 2a: Are those values averaged over the simulation domain ? over Greenland ? I had hard time to figure out how those values could be realistic. I think there is either a issue with the unit or a mistake in the calculation. Shouldn't it be ng/m3 or ng/kg instead of ug/m3 ? The total concentrations of BC in the domain should be calculated as the volume average of the grid cell concentrations, not the sum over all grid cells in the domain...
Response: We thank the reviewer for this comment that we have now corrected. We now present the average vertical concentrations over Greenland from the 2017 fires in pg/m3 in the updated Figure 2.

Fig 2b : Here again, there is an issue with the unit. The color bar indicates ug/m2 (which is probably right), but the caption says ng/m2. Which one is correct ?
Response: We also appreciate reviewer's help to correct this mistake. The error was in the legend and it has now been updated.

Fig. 4 : It is extremely difficult to see the colored grid cells an read their values. Please improve the quality of this figure.
Response: Quality of the figures has been set to 300 dpi. This should solve the problem.

Fig. 5 : Does the altitude represent agl or amsl ? The orography in Greenland is not flat.
Response: It is agl altitude and we now clarify it in the legend.

Fig 5 : Why do you keep the contribution of fires burning outside Greenland but exclude the BC contribution of anthropogenic sources ? According to Fig. 4, their contribution is absolutely not negligible and they might modify the time series of column-integrated BC in Greenland.
Response: We thank the reviewer for this comment. We tried to put also anthropogenic BC in these time-series. Column-ntegrated anthropogenic BC is very low and a stacked

line does not show anything in the time-series and that's the reason that we decided not to present it. We have added a small comment in the legend.

Fig. 6 : it would be better to use the same scale for longitude and altitude on panels (b) and (d).
Response: The reason that we did not use the same scale for longitude and altitude in these two figures is due to the small aerosol structure at high altitudes seen in the CALIOP data. We thought that this is likely due to the N. American fires that were burning at the same time with the Greenland ones. This is visible from the AOD measurements at many of the Greenland stations where large increases in AOD were observed.
In a previous comment for the AOD increase in the Narsarsuaq station at the beginning of September, we provided relevant footprint emission sensitivities and biomass burning emissions from CAMS_GFAS (see Figure R2). They explicitly show that the largest footprint was found in Canada in areas with large biomass burning emissions. However, since we do not study the impact of the N. American fires in detail, the sentences about the presence of N. American fire plumes at high altitudes in section 4.1 are rather speculative and we have removed them. We have also corrected Figure 6, as the reviewer suggested and for this, we acknowledge him.

Fig. 7c : Is the snow albedo reduction plotted for 31 August or for the full period ?
Response: The snow albedo reduction due to BC deposition from the beginning of the fires until 31 August is plotted in Figure 7c (please see last paragraph of section 4). Legend has also been updated.

Table 1 : This table is not commented nor anlyzed in text. We can notice changes in the sources of RS data at different periods, which should be detailed in the methodology section.
Response: In line 105 we state that we used different RS data to better delineate fire perimeters and define burn severity. Which day each RS tool was used is shown by pointing to Table 1. In addition, discussion of the results presented in Table 1 is presented in section 3.1 and 3.2.

Legrand, M., et al. (2016), Boreal ïnˇA̧re records in Northern Hemisphere ice cores: A review, Clim. Past, 12(10), 2033–2059.
Polashenski, C. M., J. E. Dibb, M. G. Flanner, J. Y. Chen, Z. R. Courville, A. M. Lai, J. J. Schauer, M. M. Shafer, and M. Bergin (2015), Neither dust nor black carbon causing apparent albedo decline in Greenland's dry snow zone: Implications for MODIS C5 sur-faceïnˇCˊectance,Geophys.Res.Lett.,42,9319–9327,doi:10.1002/2015GL065912.
Thomas, J. L., et al. (2017), Quantifying black carbon deposition over the Green- land ice sheet from forest fires in Canada, Geophys. Res. Lett., 44, 7965–7974, doi:10.1002/2017GL073701.

Technical comments :
L350 : "adopted". Do you mean "adapted" ?
Response: In this sentence we think that "adopted" fits better. We just used active fires from MODIS; we did not adapt anything.

L394 : Replace "for validating" by "to validate".

Response: Corrected.

L485 : Replace "attenuation" by "attenuated"
Response: Corrected.

L512 : Please write "Brent Holben" in two words.
Response: Corrected.

REFERENCES

Holben, B. N., Eck, T. F., Slutsker, I., Smirnov, A., Sinyuk, A.,Schafer, J., Giles, D., and Dubovik O.: AERONET's Version 2.0 quality assurance criteria, http://aeronet.gsfc.nasa.gov/new_web/Documents/AERONETcriteria_final1.pdf, 2006.

Andrews, E., Ogren, J. A., Kinne, S., and Samset, B.: Comparison of AOD, AAOD and column single scattering albedo from AERONET retrievals and in situ profiling measurements, Atmos. Chem. Phys., 17, 6041-6072, https://doi.org/10.5194/acp-17-6041-2017, 2017.

Dubovik, O., Smirnov, A., Holben, B. N., King, M. D., Kaufman, Y. J., Eck, T. F., and Slutsker, I.: Accuracy assessment of aerosol optical properties retrieval from AERONET sun and sky radiance measurements, J. Geophys. Res., 105, 9791–9806, 2000.

Paugam, R., Wooster, M., Atherton, J., Freitas, S. R., Schultz, M. G., and Kaiser, J. W.: Development and optimization of a wildfire plume rise model based on remote sensing data inputs – Part 2, Atmos. Chem. Phys. Discuss., 15, 9815-9895, https://doi.org/10.5194/acpd-15-9815-2015, 2015.
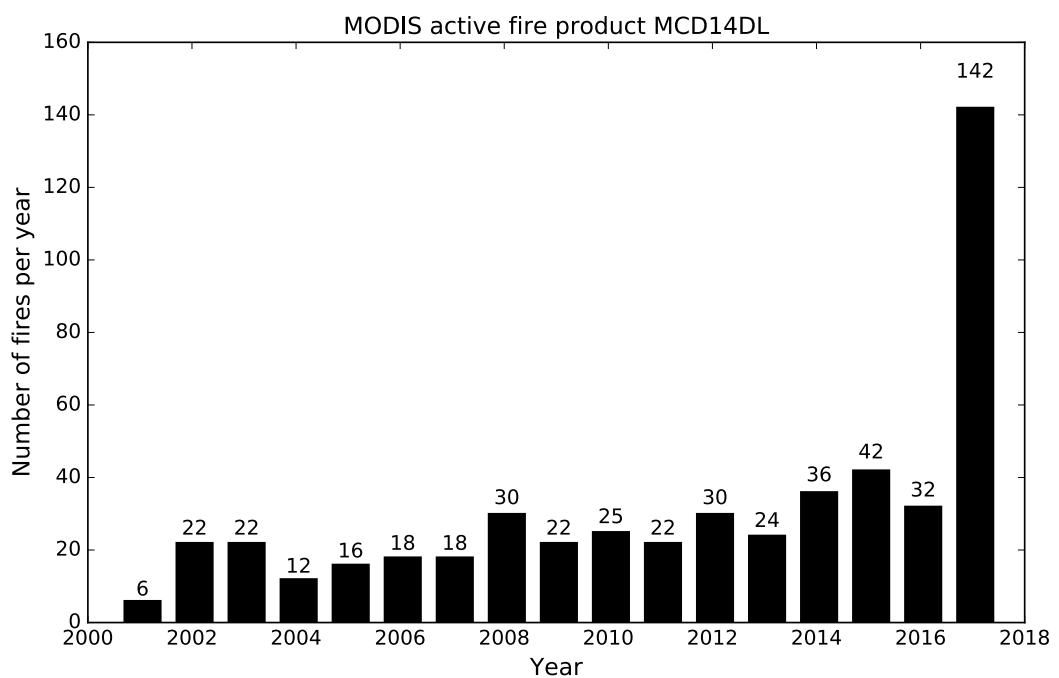
Fig. R 1. Annual number of active fires over Greenland during the last 17 years as seen from NASA's MODIS satellite (product MSC14DL).
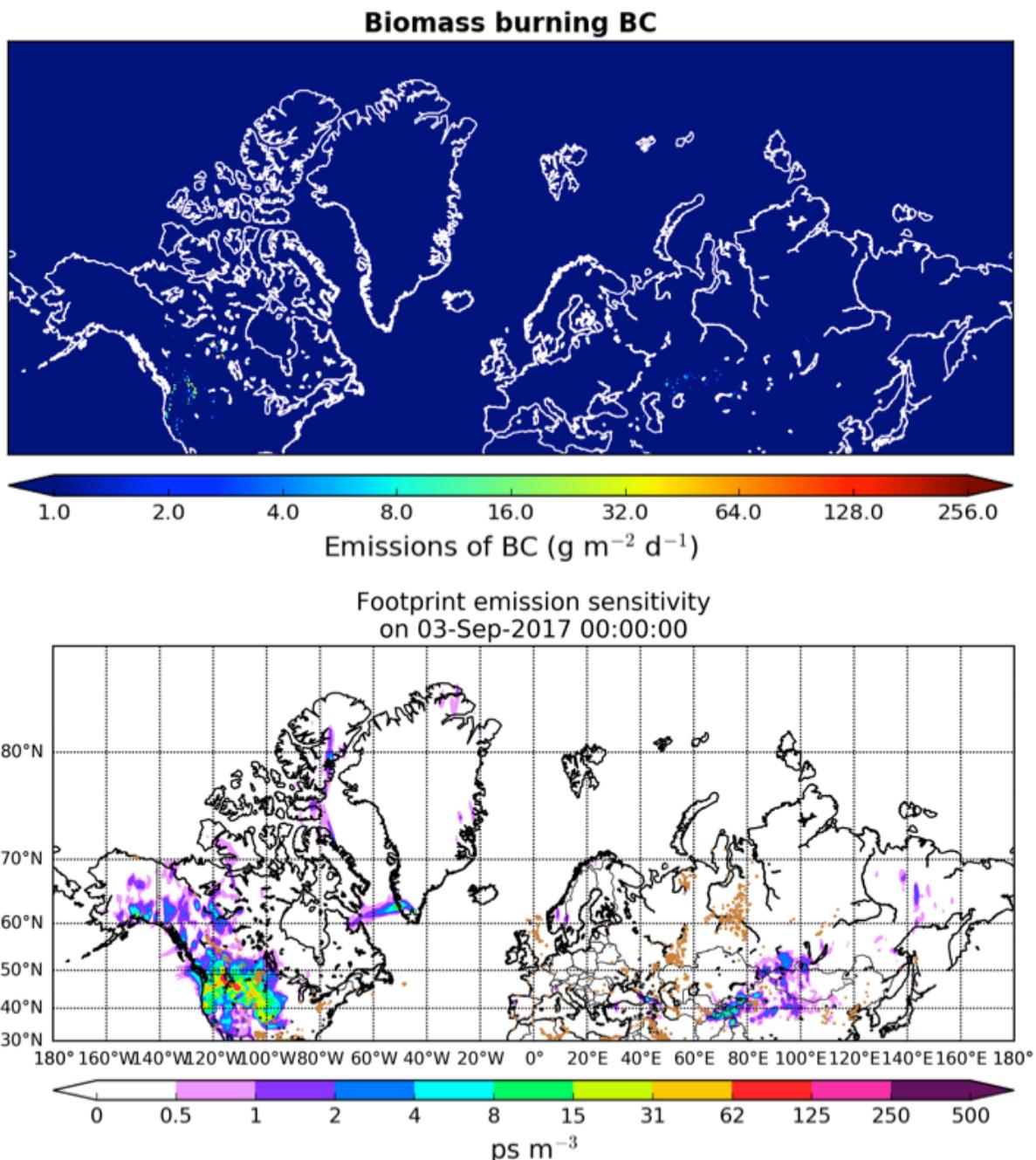
Fig. R 2. Biomass burning emissions of BC from GFAS (upper panel) in the beginning of September and the footprint emission sensitivity from the Narsarsuaq station (bottom panel) on September 3rd. The highest emission probability fits exactly to the place where the highest emissions occurred.

Open fires in Greenland in summer 2017: transport and deposition of BC and impact on the Greenland Ice Sheet

Nikolaos Evangeliou[1,*], Arve Kylling[1], Sabine Eckhardt[1], Viktor Myroniuk[2], Kerstin Stebel[1], Ronan Paugam[3], Sergiy Zibtsev[2], Andreas Stohl[1]

[1]Norwegian Institute for Air Research (NILU), Department of Atmospheric and Climate Research (ATMOS), Kjeller, Norway.

[2]National University of Life and Environmental Sciences of Ukraine, Kiev, Ukraine.

[3]King's College London, London, United Kingdom.

* Corresponding author: N. Evangeliou (Nikolaos.Evangeliou@nilu.no)

1

Abstract

Highly unusual open fires burned in Western Greenland between 31 July and 21 August 2017, after a period of warm, dry and sunny weather. The fires burned on peat lands that became vulnerable to fires by permafrost thawing. We used several satellite data sets to estimate that the total area burned was about 2345 hectares. Based on assumptions of typical burn depths and BC emission factors for peat fires, we estimate that the fires consumed a fuel amount of about 117 kt C and produced BC emissions of about 23.5 t. We used a Lagrangian particle dispersion model to simulate the atmospheric BC transport and deposition. We find that the smoke plumes were often pushed towards the Greenland Ice Sheet by westerly winds and thus a large fraction of the BC emissions (7 t or 30%) was deposited on snow or ice covered surfaces. The calculated BC deposition was small compared to BC deposition from global sources, but not entirely negligible. Analysis of aerosol optical depth data from three sites in Western Greenland in August 2017 showed strong influence of forest fire plumes from Canada, but little impact of the Greenland fires. Nevertheless, CALIOP lidar data showed that our model captured the presence and structure of the plume from the Greenland fires. The albedo changes and instantaneous surface radiative forcing in Greenland due to the fire BC emissions were estimated with the SNICAR model and the uvspec model from the libRadtran radiative transfer software package. We estimate that the maximum albedo change due to the BC deposition was about 0.006, too small to be measured. The average instantaneous surface radiative forcing over Greenland at noon on 31 August was 0.03 W m^{-2}, with locally occurring maximum values of 0.63 W m^{-2}. The average value is at least an order of magnitude smaller than the radiative forcing due to BC from other sources. Overall, the fires burning in Greenland in summer of 2017 had little impact on BC deposition on the Greenland Ice Sheet, causing almost negligible extra radiative forcing. This was due to the – in a global context – still rather small size of the fires. However, the very large fraction of the BC emissions deposited on the Greenland Ice Sheet makes these fires very efficient climate forcers on a per unit emission basis. If the expected future warming of the Arctic produces more severe fires in Greenland, this could indeed cause albedo changes and thus contribute to accelerated melting of the Greenland Ice Sheet. The fires burning in 2017 may be a harbinger of such future events.

2

1 Introduction

In August 2017 public media reported unprecedented fire events in Western Greenland (BBC News, 2017; New Scientist Magazine, 2017). These events were documented with airborne photographs (SERMITSIAQ, 2017) and satellite images (NASA, 2017b) and raised public concerns about the effects of climate change and possible impacts of soot emissions on ice melting. Historically, wildfires have occurred infrequently on Greenland, because three-quarters of the island is covered by a permanent ice sheet and permafrost is found on most of the ice-free land (Abdalati and Steffen, 2001). Permafrost, or permanently frozen soil, lies under a several meters thick "active" soil layer that thaws seasonally. But in certain areas, where the permafrost layer starts melting, it can expose peat, a material consisting of only partially decomposed vegetation that forms in wetlands over the course of hundreds of years or longer. Peatlands, also known as bogs and moors, are the earliest stage in the formation of coal. Globally, the amount of carbon stored in peat exceeds that stored in vegetation and is similar in size to the current atmospheric carbon pool (Turetsky et al., 2014). When peatlands dry, they are often affected by fires burning into the peat layers. Peat fires are difficult to extinguish and they often burn until all the organic matter is consumed. Smoldering peat fires already are the largest fires on Earth in terms of their carbon footprint (Turetsky et al., 2014). For Greenland, it has been suggested that degradation of peat will accelerate towards 2080 (Daanen et al., 2011) and that the area affected by the fires in August 2017 is particularly vulnerable to permafrost thawing (Daanen et al., 2011).

Fires in the high northern latitudes release significant amounts of CO_2, CH_4, N_2O and black carbon (BC), and their emissions are often transported into Arctic regions (Cofer III et al., 1991; Hao et al., 2016; Hao and Ward, 1993; Shi et al., 2015). BC is the most strongly light-absorbing component of the atmospheric aerosol (Bond et al., 2013) and is formed by the incomplete combustion of fossil fuels, biofuels, and biomass. It is important due to its human health (Lelieveld et al., 2015) and climate impacts (Sand et al., 2015), and its atmospheric lifetime of 3–11 days (Bond et al., 2013) facilitates transport over long distances (Forster et al., 2001; Stohl et al., 2006). BC from mid-latitude sources can thus reach remote areas such as the Arctic. BC absorbs solar radiation in the atmosphere and has a significant impact on cloud formation. It also decreases surface albedo when deposited on ice and snow and can accelerate melting processes (Hansen and Nazarenko, 2004). This raises particular concerns about the effect of fires burning in the immediate vicinity of the Greenland Ice Sheet. If a large fraction of the BC emitted by such fires is deposited on the ice, these fires

3

92 may be extremely effective in further enhancing the already accelerating melting of the
93 Greenland Ice Sheet (AMAP, 2017). BC emissions from such high latitude fires may also
94 have a substantial effect on the albedo of sea ice.

95   Here we study transport and deposition of BC over the Greenland Ice Sheet from the
96 fires that occurred in Western Greenland in August 2017, which likely represent the largest
97 fires that have occurred on Greenland in modern times (Figure S 1). Since the fires occurred
98 in an area entirely lacking ground-based observations, we use satellite data and a Lagrangian
99 atmospheric dispersion model for our study.

2 Methods

2.1 Definition of burned area

102   Remote sensing has been useful for delineating fire perimeters, characterizing burn
103 severity and planning post-fire restoration activities in different regions. The use of satellite
104 imaging is particularly important for fire monitoring in remote areas due to difficult ground
105 access. The method that is presented in this section has been already used to calculate burned
106 area in the highly-contaminated radioactive forests of Chernobyl (Evangeliou et al., 2014,
107 2015, 2016). Coordinates of fire locations (hot spots) were downloaded from FIRMS (Fire
108 Information for Resource Management System) (NASA, 2017a). For the mapping of the
109 burned area, Sentinel 2A images were used. To delineate fire perimeters and define burn
110 severity precisely, we used Landsat 8 Operational Land Imager (OLI) (resolution: 30×30 m)
111 together with Sentinel 1A (resolution: 30×30 m) and Sentinel 2A images (resolution: 30×30
112 m) (see Table 1) by applying the differenced Normalized Burn Ratio (dNBR) (Key and
113 Benson, 2006):

114 $$dNBR = NBR_{pre-fire} - NBR_{post-fire} \qquad (\text{Eq. 1})$$

115 Normalized burn ratios for pre- ($NBR_{pre-fire}$) and postfire ($NBR_{post-fire}$) images from
116 Sentinel 2A can be calculated using radiances for near- and shortwave infrared bands (bands 8
117 (NIR) and 12 (SWIR2) at 0.835 μm and 2.202 μm, respectively):

118 $$NBR = \frac{1000 \cdot (NIR - SWIR2)}{NIR + SWIR2} \qquad (\text{Eq. 2})$$

119 The methodology of applying a dNBR index to assess the impact of fires has been used in
120 forests of the Northern and Western USA (French et al., 2008; Key and Benson, 2006) and
121 elsewhere (Escuin et al., 2008; Sunderman and Weisberg, 2011).

4

125　　　　The burned severity mosaics were created using Sentinel 2A images corrected for
126　atmospheric scattering (see Chavez, 1988). Pre– and post–fire images were used to create
127　cloudless mosaics for the area where the Greenland fires burned. A Maximum Value
128　Composite (MVC) procedure (Holben, 1986) was used to select pixels from each band that
129　were not cloud covered and have a high value of Normalized Difference Vegetation Index
130　(NDVI). To avoid spurious burn severity values, manually delineated fire perimeters were
131　applied and all areas outside were classified as unburned. We have used common dNBR
132　severity levels (Key and Benson, 2006) that are presented in Figure 1. The occasionally dense
133　cloud cover was the main obstacle in reconstructing fire dynamics. As an independent source
134　of information, active fires from MODIS satellite product MCD14DL (Giglio et al., 2003) are
135　plotted in Supplemental Information (SI) Figure S 2.

2.2　Injection altitudes, assumptions on biomass consumption and emissions factors

138　　　　Injection heights into the atmosphere of the emitted smoke were simulated with version
139　2 of the Plume Rise Model (PRM) (Paugam et al., 2015) which is implemented in the Global
140　Fire Assimilation System (GFAS) emission inventory (Rémy et al., 2017). The model
141　(hereafter referred to as PRMv2) is a further development of PRM (Freitas et al., 2006, 2010)
142　and has already been used in previous studies of fire events (Evangeliou et al., 2015, 2016).
143　The model simulates a profile of smoke detrainment for every single fire, from which two
144　metrics are extracted: (i) a detrainment layer (i.e. where the detrainment rate is > 50% of its
145　global maximum) and (ii) an injection height (InjH, the top of the detrainment layer). Instead
146　of using the GFAS product, which uses the same statistics as in the PRMv2 InjH calculation,
147　we ran the model for every detected fire assuming a 6 h persistence and using the same
148　conversion factor as Kaiser et al. (2012) to estimate the biomass consumption. PRMv2 mass
149　detrainment profiles are then time integrated and extracted at $1° \times 1°$ spatial resolution with a
150　500 m vertical mesh to estimate the 3D distribution of biomass burning smoke injection into
151　the atmosphere. Figure S 3 (SI) shows for all fires recorded in the MODIS fire product
152　(Justice et al., 2002) during the fire period (31 July – 21 August 2017) the horizontal
153　distribution of the median height of the emitted smoke and its integration over the longitude
154　(right panel). Fires in Greenland showed a maximum injection height of around 2 km, but
155　according to PRMv2 the majority of the emissions (90%) remained below 800 m. Low
156　injection heights mostly inside the daytime planetary boundary layer are quite typical for
157　smoldering fires including peat fires (Ferguson et al., 2003) such as those burning in

5

Nikolaos Evangeliou 28/5/2018 14:03
Deleted: Additional classification rules were imposed t

Andreas Stohl 16/6/2018 23:00
Deleted: map burn severity more precisely

Nikolaos Evangeliou 28/5/2018 14:03
Deleted: due to the sensitivity of NBR to changes in vegetation and soil moisture. M

Nikolaos Evangeliou 21/6/2018 20:09
Deleted: Figure 1

Nikolaos Evangeliou 18/6/2018 09:31
Deleted: These confirm our results.

Andreas Stohl 16/6/2018 23:06
Deleted: burned

Nikolaos Evangeliou 21/6/2018 20:09
Deleted: Figure S 3

Andreas Stohl 16/6/2018 23:07
Deleted: biomass

168   Greenland (see below). For modeling the dispersion of BC released from the Greenland fires,
169   the emission profiles from PRMv2 were ingested into the Lagrangian particle dispersion
170   model FLEXPART (see section 2.3).

171   Wildfires in boreal peatlands in the Canadian Arctic and in Alaska typically have
172   (shallow) burn depths of 1–10 cm and consume 20–30 t C ha^{-1} (Benscoter and Wieder, 2003;
173   Shetler et al., 2008). The consumed carbon is often re-sequestered in 60–140 years after the
174   fire (Turetsky et al., 2011; Wieder et al., 2009). Given that fire return intervals can be as short
175   as 100–150 years in sub-humid continental peatlands (Wieder et al., 2009), and may exceed
176   2000 years in humid climates (Lavoie and Pellerin, 2007), northern peatlands are generally
177   resilient to wildfire (Magnan et al., 2012). For example, in peatlands of Northern Russia,
178   organic matter available for combustion has been estimated to be 121.8 t C ha^{-1} for forested
179   lands and 21.3 t C ha^{-1} for non-forested lands (Smirnov et al., 2015). Accordingly, a severe
180   wildfire that burned within an afforested peatland in the Scottish Highlands during the
181   summer of 2006 had a mean depth of burn of 17.5±2.0 cm (range: 1–54 cm) and a carbon loss
182   of 96±15 t C ha^{-1} (Davies et al., 2013). In contrast, tropical peatlands can have deep burn
183   depths of 40–50 cm and release an average of 300–450 t C ha^{-1} (Page et al., 2015; Reddy et
184   al., 2015). In the present study, we assume an average amount of organic fuel available for
185   combustion for the Greenland peat fires of August 2017 of 100 t C ha^{-1}, guided by values
186   suggested elsewhere (Smirnov et al., 2015).

187   Estimation of the emissions of BC, E_{BC} (kg), was based on the following formula
188   (Seiler and Crutzen, 1980; Urbanski et al., 2011) using the calculated burned area A (ha) and a
189   number of assumptions:

190    $$E_{BC} = A \times FL \times \alpha \times EF \qquad \text{Eq. 1}$$

191   Here, FL is the mass of the fuel available for combustion (kg C ha^{-1}); α is the dimensionless
192   combustion completeness, which was adopted from Hao et al. (2016) for litter and duff fuels
193   (50%) and EF is the emission factor of BC (kg kg^{-1}) that was adopted from Akagi et al.
194   (2011) for peatland fires (0.0002 kg kg^{-1}). Fuel consumption is calculated as the product of
195   burned area, fuel loading and combustion completeness ($A \times FL \times \alpha$).

2.3 Atmospheric modeling

197   The emissions of BC obtained from Eq. 1 were fed to the Lagrangian particle dispersion
198   model FLEXPART version 10.2 (Stohl et al., 2005) to simulate BC transport and deposition.
199   This model was originally developed for calculating the dispersion of radioactive material

Andreas Stohl 16/6/2018 23:09
Deleted: , which

Andreas Stohl 16/6/2018 23:11
Deleted: The

Andreas Stohl 16/6/2018 23:13
Moved (insertion) [2]

Andreas Stohl 16/6/2018 23:14
Deleted:

Andreas Stohl 16/6/2018 23:11
Deleted: from peat fires in Greenland were calculated fromus

Nikolaos Evangeliou 28/5/2018 14:04
Deleted: ing

Andreas Stohl 16/6/2018 23:13
Formatted: Font:Italic

Andreas Stohl 16/6/2018 23:14
Deleted: where E_{BC} is the BC emission from the fire (kg); A is the burned area (ha);

Andreas Stohl 16/6/2018 23:13
Moved up [2]: E_{BC}

209 from nuclear emergencies, but since then it has been used for many other applications (e.g.,
210 Fang et al., 2014; Stohl et al., 2011, 2013). The model has a detailed description of particle
211 dispersion in the boundary layer and a convection scheme to simulate particle transport in
212 clouds (Forster et al., 2007). The model was driven by hourly 0.5°×0.5° operational analyses
213 from the European Centre for Medium-Range Weather Forecasts (ECMWF). Concentration
214 and deposition fields were recorded in a global domain of 1°×1° spatial resolution with three
215 hourly outputs. To capture the spatiotemporal variability of BC over the Greenland Ice Sheet,
216 a nested domain with 0.05°×0.05° resolution was used. The simulations accounted for wet
217 and dry deposition, assuming a particle density of 1500 kg m^{-3} and a logarithmic size
218 distribution with an aerodynamic mean diameter of 0.25 μm and a standard deviation of 0.3
219 (Long et al., 2013). The wet deposition scheme considers below-cloud and in-cloud
220 scavenging separately based on cloud liquid water and cloud ice content, precipitation rate
221 and cloud depth from ECMWF, as described in Grythe et al. (2017).

222 To compare BC concentrations in Greenland due to the emissions of the Greenland fires
223 to those due to BC emissions occurring elsewhere, we used the so-called "retroplume" mode
224 of FLEXPART for determining the influence of other sources. For only a few receptor points,
225 this mode is computationally more efficient than forward simulations. Computational
226 particles were tracked 30 days back in time from four receptor regions: Northwestern (-62°E
227 to -42°E, 72°N to 83°N), Southwestern (-62°E to -42°E, 61°N to 72°N), Northeastern (-42°E
228 to -17°E, 72°N to 83°N) and Southeastern Greenland (-42°E to -17°E, 61°N to 72°N). The
229 retroplume mode allowed identification of the origin of BC through calculated footprint
230 emission sensitivities (often also called source-receptor relationships) that express the
231 sensitivity of the BC surface concentration at the receptor to emissions on the model output
232 grid. If these emissions are known, the BC concentrations at the receptor can be calculated as
233 the product of the emission flux and the emission sensitivity. Also, detailed source
234 contribution maps can be calculated, showing which regions contributed to the simulated
235 concentration. For the anthropogenic emissions, we used the ECLIPSE (Evaluating the
236 CLimate and Air Quality ImPacts of ShortlivEd Pollutants) version 5 (Klimont et al., 2017)
237 emission data set. For the biomass burning emissions outside Greenland, we used operational
238 CAMS GFAS emissions (Kaiser et al., 2012).

239 **2.4 Radiative forcing calculations**
240 The radiative forcing (RF) of the emitted BC was calculated using the uvspec model from the
241 libRadtran radiative transfer software package (http://www.libradtran.org/doku.php)

7

(Emde et al., 2016; Mayer and Kylling, 2005). The radiative transfer equation was solved in the independent pixel approximation using the DISORT model in pseudo-spherical geometry with improved treatment of peaked phase functions (Buras et al., 2011; Dahlback and Stamnes, 1991; Stamnes et al., 1988). Radiation absorption by gases was taken from the Kato et al. (1999) parameterization modified as described in the libRadtran documentation and Wandji Nyamsi et al. (2015). External mixture of aerosols was assumed, i.e. BC was treated in isolation of other aerosol types that may also have been present in the plume. This assumption likely leads to underestimates of the radiative impacts of BC in the atmosphere as coating, for example, can enhance the radiative effects of BC. However, these assumptions should have little impact on the more important albedo calculations (see below).For snow-covered surfaces, deposited BC was assumed to reside in the uppermost 5 mm. Below 5 mm the snow was assumed to be without any impurities. The albedo of the snow was calculated with the SNICAR model (http://snow.engin.umich.edu/info.html) in a two-layer configuration (Flanner et al., 2007, 2009).

We calculated both the bottom of the atmosphere (BOA) and top of atmosphere (TOA) instantaneous radiative forcing (IRF) due to the Greenland fires at 1°×1° resolution. The IRF includes both the effects of atmospheric BC and BC deposited on the snow. Note that the IRF does not include any semi-direct nor indirect effects. We also calculated IRF for both cloudless and cloudy conditions. IRF for cloudless conditions indicates the maximum possible effect of BC due to the fires irrespective of the actual meteorological situation, while IRF for cloudy conditions is representative of the actual conditions. For the latter, liquid and ice water clouds were adopted from ECMWF.

2.5   Remote sensing of the smoke plume

To confirm the presence of BC from fires in Greenland and elsewhere in the atmosphere over Greenland, we used the AERONET (AErosol RObotic NETwork) data (Holben et al., 1998). AERONET provides globally distributed observations of spectral aerosol optical depth (AOD), inversion products, and precipitable water in diverse aerosol regimes. We chose data from three stations that were close to the 2017 fires and for which cloud-free data exist for most of the simulated period, namely Kangerlussuaq (50.62°W–66.99°N), Narsarsuaq (45.52°W–61.16°N) and Thule (68.77°W–76.51°N). Their locations are shown in Figure S 2. We used Level 2.0 AOD data (fine and coarse mode AOD at 500 nm and total AOD at 400 nm) from the AERONET version 3 direct-sun spectral deconvolution algorithm (SDA version

8

Margin comments:

Andreas Stohl 17/6/2018 14:43
Moved (insertion) [3]

Andreas Stohl 17/6/2018 14:42
Deleted: Liquid water and ice water clouds were adopted from ECMWF operational analysis data. No aerosols except those emitted from the Greenland fires were included. As such, the RF calculations represent a maximum estimate of the effect of BC from the Greenland fires.

Andreas Stohl 17/6/2018 14:43
Moved up [3]: The radiative transfer equation was solved in the independent pixel approximation using the DISORT model in pseudo-spherical geometry with improved treatment of peaked phase functions (Buras et al., 2011; Dahlback and Stamnes, 1991; Stamnes et al., 1988). Radiation absorption by gases was taken from the Kato et al. (1999) parameterization modified as described in the libRadtran documentation and Wandji Nyamsi et al. (2015).

Andreas Stohl 17/6/2018 14:45
Deleted: . ...[1]

Nikolaos Evangeliou 21/6/2018 20:09
Deleted: Figure S 2

Nikolaos Evangeliou 30/5/2018 15:47
Deleted: display

Nikolaos Evangeliou 21/6/2018 19:22
Deleted: at 00 nm

4.1) product (downloaded on 20/06/2018) for the simulated period (31 July to 31 August 2017).

To examine in particular the vertical depth of the smoke, we used data from the CALIOP (Cloud-Aerosol Lidar with Orthogonal Polarization) lidar on the CALIPSO (Cloud-Aerosol Lidar and Infrared Pathfinder Satellite Observations) platform (Winker et al., 2009). CALIOP provides profiles of backscatter at 532 nm and 1064 nm, as well as the degree of the linear polarization of the 532 nm signal. For altitudes below 8.3 km lidar profiles at 532 nm are available with a vertical resolution of 30 m. We have utilized the level 1 data products (version 3.40) of total attenuated backscatter at 532 nm. This signal responds to aerosols (like BC) as well as water and ice clouds, which in most cases can be distinguished based on their differences in optical properties. The data were downloaded via ftp from the ICARE Data and Services Center (http://www.icare.univ-lille1.fr/).

3 Results

3.1 Indications of early permafrost degradation and fuel availability

Table 1 reports burned areas in August 2017 calculated for Greenland. In total, 2345 hectares burned between 31 July and 21 August 2017 (Figure 1). We estimate that about 117 kt of carbon were consumed by these fires. The area burned is not large compared to the global area burned each year of 464 million hectares, or the areas burned in boreal North America (2.6 million hectares) or boreal Asia (9.8 million hectares) (Randerson et al., 2012), but still highly unusual for Greenland.

It is not yet known how these fires started. Fires on carbon-rich soils can be initiated by an external source, e.g. lightning, flaming wildfire and firebrand, or self-heating. The fires burned relatively close to the town of Sisimut, so it is quite possible that humans started the fires. Self-heating is another possibility as porous solid fuels can undergo spontaneous exothermic reactions in oxidative atmospheres at low temperatures (Drysdale, 2011; Restuccia et al., 2017b). This process starts by slow exothermic oxidation at ambient temperature, causing a temperature increase, which is determined by the imbalance between the rate of heat generation and the rate of heat losses (Drysdale, 2011). Fire initiated by self-heating ignition is a well-known hazard for many natural materials (Fernandez Anez et al., 2015; Restuccia et al., 2017a; Wu et al., 2015) and can also occur in natural soils (Restuccia et al., 2017b). Southwestern Greenland was under anticyclonic influence during the last week

9

of July and according to the MODIS ESDIS worldview tool, direct sunshine occurred for eight consecutive days before the fires started at the end of July 2017. It might be possible that this long period of almost continuous insolation at these latitudes in July heated the soil enough to self-ignite. In any case, the continuous sunshine had dried the soil, making it susceptible to fire.

The fact that these fires were burning for about three weeks but spread relatively slowly compared to above-ground vegetation fires indicates that the main fuel was probably peat. The predominant vegetation in Western Greenland varies from carbon-rich Salix glauca low shrubs (mean canopy height: 95 cm), mainly at low altitude south-facing slopes with deep soils and ample moisture, to dwarf-shrubs and thermophilous graminoid vegetation (Arctic steppe) at higher altitudes (Jedrzejek et al., 2013). In addition, the observed smoke was nearly white, indicating damp fuel, such as freshly thawed permafrost, which produces smoke rich in organic carbon (OC) aerosol (Stockwell et al., 2016). Notice that while OC is not strongly absorbing, it may contain some absorbing brown carbon, which would add to the albedo reduction of snow by BC. On the other hand, BC emission factors are relatively low for peat fires (see Akagi et al., 2011).

Literally no fires should be expected in Greenland, since there is little available fuel as it has been suggested by global models and validated by observations (Daanen et al., 2011; Stendel et al., 2008); the only way to provide substantial amounts of fuel in Greenland is permafrost degradation. However, it has been suggested that significant permafrost loss in Greenland may occur only by the end of the 21st century (Daanen et al., 2011; Stendel et al., 2008). The fires in 2017 might indicate that significant permafrost degradation has occurred sooner than expected.

3.2 Transport and deposition of BC in Greenland

We estimate that about 23.5 t of BC were released from the Greenland fires in August 2017 (Table 1). According to the FLEXPART model simulations, these emissions were transported and deposited as shown in Figure 2. Due to the low injection altitude of the releases within the boundary layer, transport was relatively slow and thus most BC initially remained quite close to its emission source. Slow transport was also favored by mostly anticyclonic influence during the first half of August. It seems that even though katabatic winds from the Greenland Ice Sheet occasionally transported the plume westwards, most of the time the large-scale circulation pushed the plume back towards Greenland. Consequently, a large fraction of the emitted BC was deposited in Southwestern Greenland. On 3 August a

10

small portion of the emitted BC (≈516 kg) was lifted higher into the atmosphere and was transported to the east and deposited in the middle of the Ice Sheet over the course of the following two days (4 and 5 August). From 5 to 8 August, when the fires were particularly intense, BC was transported to the south, where most of it was deposited at the southern part of the Ice Sheet and close to the coastline. At the same time, another branch of the plume was moving to the north depositing BC over Greenland's western coastline up to 80°N. Around 10 August, the plume circulated north- and then eastwards in the northwestern sector of the anti-cyclone and BC was deposited to the northern part of the Ice Sheet until 13 August. From around 16 August, a cyclone approached from the northwest and the smoke was briefly transported directly eastwards along the southern edge of the cyclone. Strong rain associated with the cyclone's frontal system appears to have largely extinguished the fire by 17 or 18 August, although smaller patches may have continued smoldering for a few more days before they also died out. The exact fire behavior after 16 August is difficult to determine because of frequent dense cloud cover. However, satellite imagery on 21 August shows no smoke anymore in the area where the fires had burned.

The total deposition of BC from the fires in Greenland is shown in Figure 2b. About 9 t of the 23.5 t of BC emitted (or about 39%) were deposited over Greenland. About 7 t (30% of the total emissions) were deposited on snow or ice covered surfaces. Most of the rest was deposited in the Baffin Bay between Greenland and Canada and in the Atlantic Ocean.

With 30% of the emissions deposited on snow or ice surfaces, Greenland fires may have a relatively large efficiency for causing albedo changes on the Greenland Ice Sheet. By comparison, the respective BC deposition on snow and ice surfaces over Greenland from global emissions of BC was only 0.4% (39 kt) of the emissions. Even the total deposition of BC in the Arctic (>67°N) was only about 3% (215 kt). This indicates the high relative potential of Greenland fires to pollute the cryosphere (on a per unit emission basis), likely also giving them a particularly high radiative forcing efficiency. Considering that the projected rise of Greenland temperatures is expected to result in further degradation of the permafrost (Daanen et al., 2011) and, hence, likely resulting in more and larger peat fires on Greenland, this constitutes a potentially important climate feedback which could accelerate melting of the glaciers and ice sheet of Greenland and enhance Arctic warming.

We also calculated the concentration of the deposited BC in Greenland snow (Figure 3) by taking the ratio of deposited BC and the amount of water deposited by rain or snow fall during the same time period (31 July to 31 August 2017). As expected, BC snow

11

Andreas Stohl 17/6/2018 00:15
Deleted: , while a

Andreas Stohl 17/6/2018 00:15
Deleted: on

Nikolaos Evangeliou 21/6/2018 20:09
Deleted: Figure 2

Andreas Stohl 17/6/2018 00:17
Deleted: from the Greenland fires in summer 2017

Andreas Stohl 17/6/2018 00:17
Deleted: , which is about 39% of the fires' total emissions

Nikolaos Evangeliou 21/6/2018 20:09
Deleted: Figure 3

concentrations show the same general patterns as the simulated deposition of BC with the highest concentrations obtained close to the source. High BC in snow concentrations were also computed in some regions of the Ice Sheet due to relatively intense precipitation events. By contrast, dry deposition of BC over the Ice Sheets was low (Figure 3). Dry deposition was responsible for a major fraction of the deposition only in regions where the plume was transported during dry weather, and in most of these regions total deposition was low. A notable exception is the region close to the fires, where dry deposition was relatively important due to the generally dry weather when the fires were burning. It can be also ascribed to the fact that dry deposition occurs in the quasi-laminar sub–layer close to the surface. A fraction of the aerosols can be quickly deposited close to the sources before the they are transported to higher altitudes and away from the sources (Bellouin and Haywood, 2014). The average calculated concentration of BC on the Ice Sheet was estimated to be <1 ng g^{-1}, but in some areas snow concentrations reached up to 3 ng g^{-1}. These higher values are substantial considering that measured concentrations of BC in snow typically range up to 16 ng g^{-1} in most of Greenland (Doherty et al., 2010) or from 1 – 17 ng g^{-1} in summer 2012 and 3–43 ng g^{-1} in summer 2013 (Polashenski et al., 2015) and up to 15 ppb (ng g^{-1}) during preindustrial times (from 1740 to 1870) on average (Legrand et al., 2016).

It has been reported that the size of rapidly coagulated BC particles produced by different types of fires ranges between 0.1 to 10 µm, but more than 90% of the BC mass lies between 0.1 and 1 µm (e.g., Conny and Slater, 2002; Long et al., 2013; Zhuravleva et al., 2017 and many others). Therefore, we have chosen to simulate the Greenland fires with an aerodynamic mean diameter of 0.25 µm for BC and a logarithmic standard deviation of 0.3 (see section 2.3). To examine the sensitivity of deposition of BC in the Greenland Ice Sheet from the Greenland fires of 2017 to the particle size distribution used in the model, we simulated the same event for BC particles with aerodynamic mean diameters of 0.1, 0.25, 0.5, 1, 2, 4 and 8 µm and calculated the relative standard deviation of the deposition of BC normalized against the aerodynamic mean diameter of 0.25 µm that was our basic assumption (Figure S 4). The use of different size distributions for the BC particles produced from the 2017 fires created a relative uncertainty on the deposited mass of BC in the Greenland Ice Sheet, which ranges from 10%–30% in 86% of the Sheet's surface to up to 50% in the rest of the Sheet's surface. As expected, the calculated uncertainty is sensitive to the use of larger particles for BC; though BC particles larger than 1 µm are rather rare in peat fires (Hosseini et al., 2010; Leino et al., 2014).

Nikolaos Evangeliou 21/6/2018 20:09
Deleted: Figure 3

Andreas Stohl 17/6/2018 00:24
Deleted: mostly

Andreas Stohl 16/6/2018 11:02
Deleted: Aerosols are

Andreas Stohl 16/6/2018 11:03
Deleted: being

Andreas Stohl 16/6/2018 11:02
Deleted: injected at

Andreas Stohl 16/6/2018 11:02
Deleted: being transported

Andreas Stohl 17/6/2018 00:26
Deleted: during

Andreas Stohl 17/6/2018 00:26
Deleted: produced

Andreas Stohl 17/6/2018 00:26
Deleted: to

Nikolaos Evangeliou 21/6/2018 20:09
Deleted: Figure S 4

3.3 Impact from other emissions in Northern Hemisphere

In summertime 2017, intense wildfires were reported in British Columbia, Western Canada (NASA, 2017c), and fires also burned at mid latitudes in Eurasia, as is typical during spring and summer (Hao et al., 2016). Previous studies of wildfires have shown that the produced energy can be sufficient to loft smoke above the boundary layer by supercell convection (Fromm et al., 2005) even up to stratospheric altitudes (Leung et al., 2007). As a result, BC can become subject to long-range transport over long distances (Forster et al., 2001; Stohl et al., 2007). To examine the impact of these fires in Greenland, average footprint emission sensitivities were calculated for four compartments of Greenland (Northwestern, Southwestern, Northeastern and Southeastern Greenland) for the period 31 July to 31 August 2017 and the results are shown in Figure S 5, together with the active fires in the Northern Hemisphere from 10 July to 31 August 2017 adopted from the MODIS satellite product (MCD14DL) (Giglio et al., 2003). As can be seen in Figure S 5, fires in Alaska might have affected BC concentrations in Greenland, as the corresponding emission sensitivities are the highest in North America. On the contrary, BC emitted from fires in Eurasia seems to have affected Greenland less.

Using gridded emissions for BC, the contribution of both biomass burning and anthropogenic sources to surface BC concentrations in the four different regions over Greenland (Northwestern, Northeastern, Southwestern and Southeastern Greenland, Figure S 6) was calculated (see section 2.3). Fires affected the northern part of Greenland more than the southern part with an average concentration of about 30 ng m^{-3}, almost twice the respective average for Southern Greenland ($\approx$16 ng m^{-3}). About one third of the BC originated from wildfires in Eurasia and the rest from North America where the year 2017 appears to have been a particularly high fire year. The anthropogenic contribution to surface BC over Greenland was only about 14% to 50% of the total contribution from all biomass burning sources (Figure S 6), similar to what has been suggested previously for the Arctic in summer (Winiger et al., 2017). The anthropogenic contribution is larger in Southern Greenland than in Northern Greenland, due to the shorter distance from the main emission areas of North America and Western Europe, but it remains lower than the biomass burning contribution. The BC concentrations that are calculated here for the studied fire period (31 July to 31 August 2017) are relatively high compared to those reported previously. For instance, von Schneidemesser et al. (2009) observed an annual average BC concentration of 20 ng m^{-3} at Summit (Greenland) in 2006, while Massling et al. (2015) reported a summer

Nikolaos Evangeliou 21/6/2018 20:09
Deleted: Figure S 5

Andreas Stohl 17/6/2018 00:45
Deleted: shown

Nikolaos Evangeliou 21/6/2018 20:09
Deleted: Figure S 5

Nikolaos Evangeliou 21/6/2018 20:09
Deleted: Figure S 6

Nikolaos Evangeliou 6/6/2018 17:53
Deleted: Figure 4

Nikolaos Evangeliou 21/6/2018 20:09
Deleted: Figure S 6

Nikolaos Evangeliou 6/6/2018 17:54
Deleted: Figure 4

Nikolaos Evangeliou 31/5/2018 11:36
Deleted: In contrast to biomass burning, t

Andreas Stohl 17/6/2018 00:48
Deleted: ,

Andreas Stohl 17/6/2018 00:48
Deleted: contrast to

512 average BC concentration of 11 ng m^{-3} at station Nord (Greenland) between May 2011 and

513 August 2013. We attribute this to more active fires during 2017 than in previous years.

514   To compare how important Northern Hemispheric biomass burning emissions were for

515 the air over Greenland, we present time-series of surface BC concentrations in Northwestern,

516 Northeastern, Southwestern and Southeastern Greenland from the fires in Greenland and from

517 all the other wildfire emissions occurring outside Greenland (North Hemisphere) for the same

518 period of time (Figure 4). The calculated dosages (concentrations summed over a specific

519 time period) for the same time period were also computed. The fires in Greenland affected

520 mainly its western part with concentrations that reached up to 4.8 ng m^{-3} (Southwestern

521 Greenland on 10 August) and 4.4 ng m^{-3} (Northwestern Greenland on 12 August), while BC

522 concentrations in the eastern part remained significantly lower (Figure 4). These

523 concentrations are substantial considering that the observed surface BC concentrations in

524 Greenland in summer are usually below 20 ng m^{-3} (Massling et al., 2015). Surface BC due to

525 wildfires occurring outside Greenland was also low most of the time in the studied period (up

526 to 10 ng m^{-3} at maximum) except for a large peak between 19 and 23 August that mainly

527 affected Northern Greenland (Figure 4). The concentrations during this episodic peak were as

528 high as 27 ng m^{-3}. During the same period, the contribution from anthropogenic emissions

529 was also a few ng m^{-3} (Figure 4). BC dosages for the simulation period (31 July – 10 August

530 2017) in Western Greenland due to the Greenland fires were about one order of magnitude

531 smaller than dosages from fires elsewhere but of the same order of magnitude as BC

532 originating from anthropogenic emissions.

4 Discussion

4.1 A validation attempt

535   There are few observations available that can be used to validate our model results. We

536 use the AERONET and CALIOP data for some qualitative comparisons. Contours of

537 simulated vertical distribution of BC and column-integrated simulated BC from fires inside

538 and outside Greenland are plotted together with time-series of measured AOD (fine and

539 coarse mode AOD at 500 nm and total AOD at 400 nm) for the AERONET stations

540 Kangerlussuaq, Narsarsuaq and Thule (Figure 5). It can be seen that observed AOD variations

541 were in very good agreement with the variation of simulated column-integrated BC from fires

542 outside Greenland (mainly in Canada), confirming that the transport of these fire plumes was

543 well captured by FLEXPART. Good examples are the peaks at Kangerlussuaq on 24 August,

14

Nikolaos Evangeliou 31/5/2018 11:39
Deleted: the study period

Nikolaos Evangeliou 31/5/2018 11:39
Deleted: other

Andreas Stohl 17/6/2018 00:49
Deleted: (see Figure S 1)

Nikolaos Evangeliou 21/6/2018 20:09
Deleted: Figure 4

Nikolaos Evangeliou 6/6/2018 17:51
Deleted: Figure S 4

Nikolaos Evangeliou 21/6/2018 20:09
Deleted: Figure 4

Nikolaos Evangeliou 6/6/2018 17:52
Deleted: Figure S 4

Nikolaos Evangeliou 21/6/2018 20:09
Deleted: Figure 4

Nikolaos Evangeliou 6/6/2018 17:52
Deleted: Figure S 4

Nikolaos Evangeliou 21/6/2018 20:09
Deleted: Figure 4

Nikolaos Evangeliou 6/6/2018 17:52
Deleted: Figure S 4

Nikolaos Evangeliou 1/6/2018 15:58
Deleted: for

Nikolaos Evangeliou 1/6/2018 15:58
Deleted: ing

Nikolaos Evangeliou 21/6/2018 19:21
Deleted: at a wavelength of

Nikolaos Evangeliou 21/6/2018 20:09
Deleted: Figure 5Figure 5

559 at Narsarsuaq on 19 August and at Thule on 21 August (Figure 5) that are attributed to the
560 Canadian fires. The simulated contribution of the Greenland fires to simulated BC burdens
561 was negligible by comparison, except at Kangerlussuaq in the beginning of August when the
562 Greenland fire emissions were the highest. This station is less than 100 km away from where
563 the fires burned, but not in the main direction of the BC plume transport. It seems the period
564 of simulated fire influence corresponds to a small increase of the observed AOD values of up
565 to 20% (Figure 5).

566 To validate the smoke plume's vertical extent, we used the CALIOP data. These data
567 were only available from 5 August 2017 onward and frequent dense cloud cover inhibited
568 lidar observations at the altitudes below the clouds. High aerosol backscatter was only found
569 in the close vicinity of the fires. Figure 6a shows NASA's ESDIS view of the plume on 14
570 August 2017 at 6 UTC (available: https://worldview.earthdata.nasa.gov/?p=ge
571 ographic&l=MODIS_Aqua_CorrectedReflectance_TrueColor(hidden),MODIS_Terra_Correc
572 tedReflectance_TrueColor,MODIS_Fires_Terra,MODIS_Fires_Aqua,Reference_Labels(hidd
573 en),Reference_Features,Coastlines&t=2017-08-14&z=3&v=-
574 54.13349998138993,66.35888052399868,-50.32103113049877,69.08420005412792), where
575 a clear smoke signal was recorded. A CALIOP overpass through the edge of the plume allows
576 studying its vertical structure. Increased attenuated backscatter is found below ~1.5 km above
577 sea level between 52°E and 51°E (Figure 6b; black line denotes the orography). Figure 6c
578 (red line), shows that the CALIOP overpass transects directly the simulated plume of the
579 Greenland fires. Notice that the simulated plume also agrees very well with the smoke as seen
580 in NASA's ESDIS picture (Figure 6a). The vertical distribution of simulated BC as a function
581 of longitude is illustrated in Figure 6d. It corresponds very well to the vertical distribution of
582 aerosols observed by CALIOP (Figure 6b). In particular, the smoke resides at altitudes below
583 1.5 km and at exactly the same location both in the simulations and observations.

584 **4.2 Radiative forcing and albedo effects**
585 BOA IRF for noon on 31 August 2017 is depicted in Figure 7, both for cloudless (Fig.
586 7a) and cloudy conditions (Fig. 7b). This day is shown because almost all BC emitted by the
587 fires had been deposited before, thus giving a high IRF via albedo reduction due to BC
588 contamination of snow. For the cloudless conditions, the IRF is largest over ice close to the
589 fire site and at locations with relatively large BC deposits. The maximum IRF is 1.82 W m^{-2},
590 while the average for Greenland is 0.05 W m^{-2}. For the IRF including clouds the maximum
591 BOA (TOA) RF is 0.63 W m^{-2} (0.59 W m^{-2}), and the average 0.03 W m^{-2} (0.03 W m^{-2}).

15

Clouds are thus found to reduce the maximum BOA IRF by a factor of 2.9 and the average BOA IRF by a factor of 1.7.

The IRF depends on the optical properties of the smoke from the fire, which are not known. Hence, a sensitivity analysis was performed where the single scattering albedo (SSA) was perturbed in contrast to a "medium case" (Figure S 7a) that was adopted from the SNICAR model (Flanner et al., 2007, 2009) and has been used for the discussion in the previous paragraph. To estimate the uncertainty due to the choice of BC optical properties, additional calculations were made by scaling the SSA (red solid lines in Figure S 7a). The choices of these scaled SSA values were based on the SSA reported for various modified combustion efficiencies (MCE) by Pokhrel et al. (2016). Pokhrel et al. (2016) reported an MCE of 0.9 for peat land. As such, our adopted SSA may be considered low (compare black solid line and red line with upward triangles). Figure S 7b shows the IRF as BC is deposited for the three cases. It suggests that the IRF ranges between 40% and 130% of our above assumed medium-case values for realistic variation of the aerosol optical properties.

Figure 7d depicts the temporal behaviour of the cloudy TOA IRF averaged over Greenland (red line). In addition the daily averaged IRF is shown (green line). The daily averaged IRF is seen to increase as the plume from the fires spreads out and starts to decline after the fires were extinguished at the end of the month. The fact that the reduction towards end of August is relatively slow is caused by the effect of the albedo reduction, which persists until clean snow covers the polluted snow. Overall, albedo reduction dominates the total IRF averaged over Greenland for the period of study contributing between 85% (in the beginning of the study period) to 99% (at the end of the study period) and increasing in relative importance with time as atmospheric BC is removed.

According to Hansen et al. (2005) the TOA IRF of BC approximates the adjusted RF as reported by Myhre et al. (2013). In their Table 8.4, Myhre et al. (2013) estimated the global averaged RF due to BC between the years 1750 and 2011 to be +0.40 (+0.05 to +0.80) W m^{-2}. Skeie et al. (2011) estimated a global mean radiative forcing of 0.35 W m^{-2} due to fossil fuel and biofuel increases between 1750 and 2000. For Greenland, Skeie et al. (2011) found the RF to be less than about 0.2 W m^{-2}. This number may be compared to our area averaged IRF estimate due to the Greenland fire. For cloudy conditions the TOA IRF over Greenland due to the Greenland fires is about one order of magnitude smaller compared with the RF over Greenland due to BC from all global anthropogenic sources reported in Skeie et al. (2011).

The albedo reduction at 550 nm due to the deposited BC from the Greenland fires is shown in Figure 7c. The maximum albedo change is about 0.006. This albedo change has an

16

impact on IRF, but it is too small to be measured by satellites. For example, MODIS albedo estimates have been compared to in situ albedo measurements in Greenland by Stroeve et al. (2005). They found that the root mean square error between MODIS and in situ albedo values was ±0.04 for high quality flagged MODIS albedo retrievals. Unmanned Aerial Vehicle (UAV) measurements over Greenland made by Burkhart et al. (2017) have uncertainties of similar magnitude. Also, Polashenski et al. (2015) reported that the albedo reduction due to aerosol impurities on the Greenland Ice Sheet in 2012–2014 period is relatively small (mean 0.003), though episodic aerosol deposition events can reduce albedo by 0.01–0.02. The albedo changes due to BC from the Greenland fires are generally an order of magnitude smaller (Figure 7c) and thus too small to be detected by present UAV and satellite instruments and retrieval methods (Warren, 2013).

5   Conclusions

The conclusions from our study of the unusual open fires burning in Greenland between 31 July and 21 August 2017 are the following:

- The fires burned on peat lands that became vulnerable by permafrost thawing. The region where the fires burned was identified previously as being susceptible to permafrost melting; however, large-scale melting was expected to occur only towards the end of the 21st century. The 2017 fires show that at least in some locations substantial permafrost thawing is occurring already now.

- The total area burned was about 2345 hectares. We estimate that the fires consumed a fuel amount of about 117 kt C and produced BC emissions of about 23.5 t.

- The Greenland fires were small compared to fires burning at the same time in North America and Eurasia, but a large fraction of their BC emissions (30% or 7 t) was deposited on the Greenland Ice Sheet or glaciers.

- Measurements of aerosol optical depth at three sites in Western Greenland in August 2017 were strongly influenced by forest fires in Canada burning at the same time, but the Greenland fires had an observable impact doubling the column-integrated BC concentrations only at the closest station.

- A comparison of the simulated BC releases in FLEXPART with the vertical cross-section of total attenuated backscatter (at 532 nm) from CALIOP lidar showed that the spatiotemporal evolution and particularly the top height of the plume was captured by the model.

17

Andreas Stohl 17/6/2018 11:32
Deleted: the radiative forcing

Nikolaos Evangeliou 21/6/2018 20:09
Deleted: Figure 7Figure 7

Nikolaos Evangeliou 8/6/2018 15:13
Deleted: This BC deposition was small compared to BC deposition from global anthropogenic and biomass burning sources, but not entirely negligible.

Nikolaos Evangeliou 1/6/2018 15:59
Deleted: ion

- We estimate that the maximum albedo change due to the BC deposition from the Greenland fires was about 0.006, too small to be measured by satellites or other means. The average instantaneous BOA radiative forcing over Greenland at noon on 31 August was 0.03 W m^{-2}, with locally occurring maximum values of 0.63 W m^{-2}. The average value is at least an order of magnitude smaller than the radiative forcing due to BC from other sources.

- We conclude that the fires burning in Greenland in summer of 2017 had little impact on BC deposition on the Greenland Ice Sheet, causing almost negligible extra radiative forcing. This was due to the – in a global context - still rather small size of the fires. The very large fraction of the BC emissions deposited on the Greenland Ice Sheet (30% of the emissions) makes these fires very efficient climate forcers on a per unit emission basis. Thus, while the fires in 2017 were still relatively small on a global scale, if the expected future warming of the Arctic (IPCC, 2013) produces more and larger fires in Greenland in the future (Keegan et al., 2014), this could indeed cause substantial albedo changes and thus contribute to accelerated melting of the Greenland Ice Sheet.

Author contributions. NE performed the simulations, analyses, wrote and coordinated the paper. AK performed the radiation calculations and wrote parts of the paper. VM and SZ performed GIS analysis for the burned area calculations. RP made all the runs for the

---

Andreas Stohl 17/6/2018 11:37
Deleted: surface

Andreas Stohl 17/6/2018 11:39
Deleted: If

Nikolaos Evangeliou 25/5/2018 12:30
Deleted: further

Nikolaos Evangeliou 25/5/2018 12:30
Deleted: Greenland

Nikolaos Evangeliou 25/5/2018 15:21
Deleted: much larger

Nikolaos Evangeliou 6/6/2018 15:23
Deleted: lead

18

770	injection height calculations using the PRMv2 model. KS analysed satellite data for AOD and

771	CALIOP, SE and AS commented and coordinated the manuscript. All authors contributed to

772	the final version of the manuscript.

773
774	**References**

775	Abdalati, W. and Steffen, K.: Greenland Ice Sheet melt extent:1979-1999, J. Geophys. Res.
776	Atmos., 106(D24), 33983–33988, doi:10.1029/2001JD900181, 2001.
777	Akagi, S. K., Yokelson, R. J., Wiedinmyer, C., Alvarado, M. J., Reid, J. S., Karl, T., Crounse, J.
778	D. and Wennberg, P. O.: Emission factors for open and domestic biomass burning for use
779	in atmospheric models, Atmos. Chem. Phys., 11(9), 4039–4072, doi:10.5194/acp-11-
780	4039-2011, 2011.
781	AMAP: Snow, Water, Ice and Permafrost. Summary for Policy-makers, Arctic Monitoring
782	and Assessment Programme (AMAP), Oslo, Norway. [online] Available from:
783	https://www.amap.no/documents/doc/Snow-Water-Ice-and-Permafrost.-Summary-
784	for-Policy-makers/1532 (Accessed 27 November 2017), 2017.
785	BBC News: "Unusual" Greenland wildfires linked to peat, [online] Available from:
786	http://www.bbc.com/news/science-environment-40877099 (Accessed 6 September
787	2017), 2017.
788	Bellouin, N. and Haywood, J.: Aerosols: Climatology of Tropospheric Aerosols, Second
789	Edi., Elsevier., 2014.
790	Benscoter, B. W. and Wieder, R. K.: Variability in organic matter lost by combustion in a
791	boreal bog during the 2001 Chisholm fire, Can. J. For. Res., 33(12), 2509–2513,
792	doi:10.1139/x03-162, 2003.
793	Bond, T. C., Doherty, S. J., Fahey, D. W., Forster, P. M., Berntsen, T., Deangelo, B. J., Flanner,
794	M. G., Ghan, S., Kärcher, B., Koch, D., Kinne, S., Kondo, Y., Quinn, P. K., Sarofim, M. C.,
795	Schultz, M. G., Schulz, M., Venkataraman, C., Zhang, H., Zhang, S., Bellouin, N., Guttikunda,
796	S. K., Hopke, P. K., Jacobson, M. Z., Kaiser, J. W., Klimont, Z., Lohmann, U., Schwarz, J. P.,
797	Shindell, D., Storelvmo, T., Warren, S. G. and Zender, C. S.: Bounding the role of black
798	carbon in the climate system: A scientific assessment, J. Geophys. Res. Atmos., 118(11),
799	5380–5552, doi:10.1002/jgrd.50171, 2013.
800	Buras, R., Dowling, T. and Emde, C.: New secondary-scattering correction in DISORT with
801	increased efficiency for forward scattering, J. Quant. Spectrosc. Radiat. Transf., 112(12),
802	2028–2034, doi:10.1016/j.jqsrt.2011.03.019, 2011.
803	Chavez, P. S.: An improved dark-object subtraction technique for atmospheric scattering
804	correction of multispectral data, Remote Sens. Environ., 24(3), 459–479,
805	doi:10.1016/0034-4257(88)90019-3, 1988.
806	Cofer III, W. R., Levine, J. S., Winstead, E. L. and Stocks, B. J.: New estimates of nitrous
807	oxide emissions from biomass burning, Nature, 349(6311), 689–691 [online] Available
808	from: http://dx.doi.org/10.1038/349689a0, 1991.
809	Conny, J. and Slater, J.: Black carbon and organic carbon in aerosol particles from crown
810	fires in the Canadian boreal forest, J. Geophys. Res. … [online] Available from:
811	http://onlinelibrary.wiley.com/doi/10.1029/2001JD001528/full, 2002.
812	Daanen, R. P., Ingeman-Nielsen, T., Marchenko, S. S., Romanovsky, V. E., Foged, N.,
813	Stendel, M., Christensen, J. H. and Hornbech Svendsen, K.: Permafrost degradation risk
814	zone assessment using simulation models, Cryosphere, 5(4), 1043–1056,
815	doi:10.5194/tc-5-1043-2011, 2011.
816	Dahlback, A. and Stamnes, K.: A new spherical model for computing the radiation field

817 available for photolysis and heating at twilight, Planet. Space Sci., 39(5), 671–683,
818 doi:10.1016/0032-0633(91)90061-E, 1991.
819 Davies, G. M., Gray, A., Rein, G. and Legg, C. J.: Peat consumption and carbon loss due to
820 smouldering wildfire in a temperate peatland, For. Ecol. Manage., 308, 169–177,
821 doi:10.1016/j.foreco.2013.07.051, 2013.
822 Doherty, S. J., Warren, S. G., Grenfell, T. C., Clarke, A. D. and Brandt, R. E.: Light-absorbing
823 impurities in Arctic snow, Atmos. Chem. Phys., 10(23), 11647–11680, doi:10.5194/acp-
824 10-11647-2010, 2010.
825 Drysdale, D.: An Introduction to Fire Dynamics, 3rd Editio., John Wiley & Sons, Ltd.,
826 2011.
827 Emde, C., Buras-Schnell, R., Kylling, A., Mayer, B., Gasteiger, J., Hamann, U., Kylling, J.,
828 Richter, B., Pause, C., Dowling, T. and Bugliaro, L.: The libRadtran software package for
829 radiative transfer calculations (version 2.0.1), Geosci. Model Dev., 9(5), 1647–1672,
830 doi:10.5194/gmd-9-1647-2016, 2016.
831 Escuin, S., Navarro, R. and Fernández, P.: Fire severity assessment by using NBR
832 (Normalized Burn Ratio) and NDVI (Normalized Difference Vegetation Index) derived
833 from LANDSAT TM/ETM images, Int. J. Remote Sens., 29(4), 1053–1073,
834 doi:10.1080/01431160701281072, 2008.
835 Evangeliou, N., Balkanski, Y., Cozic, A., Hao, W. M. and Møller, A. P.: Wildfires in
836 Chernobyl-contaminated forests and risks to the population and the environment: A
837 new nuclear disaster about to happen?, Environ. Int., 73, 346–358,
838 doi:10.1016/j.envint.2014.08.012, 2014.
839 Evangeliou, N., Balkanski, Y., Cozic, A., Hao, W. M., Mouillot, F., Thonicke, K., Paugam, R.,
840 Zibtsev, S., Mousseau, T. A., Wang, R., Poulter, B., Petkov, A., Yue, C., Cadule, P., Koffi, B.,
841 Kaiser, J. W., Møller, A. P. and Classen, A. T.: Fire evolution in the radioactive forests of
842 Ukraine and Belarus: Future risks for the population and the environment, Ecol.
843 Monogr., 85(1), 49–72, doi:10.1890/14-1227.1, 2015.
844 Evangeliou, N., Zibtsev, S., Myroniuk, V., Zhurba, M., Hamburger, T., Stohl, A., Balkanski,
845 Y., Paugam, R., Mousseau, T. A., Møller, A. P. and Kireev, S. I.: Resuspension and
846 atmospheric transport of radionuclides due to wildfires near the Chernobyl Nuclear
847 Power Plant in 2015: An impact assessment., Sci. Rep., 6, 26062 [online] Available from:
848 http://www.nature.com/srep/2016/160517/srep26062/full/srep26062.html, 2016.
849 Fang, X., Thompson, R. L., Saito, T., Yokouchi, Y., Kim, J., Li, S., Kim, K. R., Park, S., Graziosi,
850 F. and Stohl, A.: Sulfur hexafluoride (SF6) emissions in East Asia determined by inverse
851 modeling, Atmos. Chem. Phys., 14(9), 4779–4791, doi:10.5194/acp-14-4779-2014,
852 2014.
853 Faulkner Burkhart, J., Kylling, A., Schaaf, C. B., Wang, Z., Bogren, W., Storvold, R., Solbø, S.,
854 Pedersen, C. A. and Gerland, S.: Unmanned aerial system nadir reflectance and MODIS
855 nadir BRDF-adjusted surface reflectances intercompared over Greenland, Cryosphere,
856 11(4), 1575–1589, doi:10.5194/tc-11-1575-2017, 2017.
857 Ferguson, S. A., Collins, R. L., Ruthford, J. and Fukuda, M.: Vertical distribution of
858 nighttime smoke following a wildland biomass fire in boreal Alaska, J. Geophys. Res.,
859 108(June), D23, 4743, doi:10.1029/2002JD003324, doi:10.1029/2002JD003324, 2003.
860 Fernandez Anez, N., Garcia Torrent, J., Medic Pejic, L. and Grima Olmedo, C.: Detection of
861 incipient self-ignition process in solid fuels through gas emissions methodology, J. Loss
862 Prev. Process Ind., 36, 343–351, doi:10.1016/j.jlp.2015.02.010, 2015.
863 Flanner, M. G., Zender, C. S., Randerson, J. T. and Rasch, P. J.: Present-day climate forcing
864 and response from black carbon in snow, J. Geophys. Res. Atmos., 112(11), 1–17,
865 doi:10.1029/2006JD008003, 2007.

866 Flanner, M. G., Zender, C. S., Hess, P. G., Mahowald, N. M., Painter, T. H., Ramanathan, V.
867 and Rasch, P. J.: Springtime warming and reduced snow cover from carbonaceous
868 particles, Atmos. Chem. Phys., 9, 2481–2497, doi:10.5194/acp-9-2481-2009, 2009.
869 Forster, C., Wandinger, U., Wotawa, G., James, P., Mattis, I., Althausen, D., Simmonds, P.,
870 O'Doherty, S., Jennings, S. G., Kleefeld, C., Schneider, J., Trickl, T., Kreipl, S., Jäger, H. and
871 Stohl, A.: Transport of boreal forest fire emissions from Canada to Europe, J. Geophys.
872 Res., 106, 22887, doi:10.1029/2001JD900115, 2001.
873 Forster, C., Stohl, A. and Seibert, P.: Parameterization of convective transport in a
874 Lagrangian particle dispersion model and its evaluation, J. Appl. Meteorol. Climatol.,
875 46(4), 403–422, doi:10.1175/JAM2470.1, 2007.
876 Freitas, S. R., Longo, K. M., Chatfield, R., Latham, D., Silva Dias, M. a. F., Andreae, M. O.,
877 Prins, E., Santos, J. C., Gielow, R. and Carvalho, J. a.: Including the sub-grid scale plume
878 rise of vegetation fires in low resolution atmospheric transport models, Atmos. Chem.
879 Phys. Discuss., 6(6), 11521–11559, doi:10.5194/acpd-6-11521-2006, 2006.
880 Freitas, S. R., Longo, K. M., Trentmann, J. and Latham, D.: Technical Note: Sensitivity of 1-
881 D smoke plume rise models to the inclusion of environmental wind drag, Atmos. Chem.
882 Phys., 10(2), 585–594, doi:10.5194/acp-10-585-2010, 2010.
883 French, N., Kasischke, E., Hall, R., Murphy, K., Verbyla, D., Hoy, E. and Allen, J.: Using
884 Landsat data to assess fire and burn severity in the North American boreal forest region:
885 an overview and summary of results, Int. J. Wildl. Fire, 17(4), 443–462,
886 doi:10.1071/WF08007, 2008.
887 Fromm, M., Bevilacqua, R., Servranckx, R., Rosen, J., Thayer, J. P., Herman, J. and Larko, D.:
888 Pyro-cumulonimbus injection of smoke to the stratosphere: Observations and impact of
889 a super blowup in northwestern Canada on 3-4 August 1998, J. Geophys. Res. D Atmos.,
890 110(8), 1–17, doi:10.1029/2004JD005350, 2005.
891 Giglio, L., Descloitres, J., Justice, C. O. and Kaufman, Y. J.: An enhanced contextual fire
892 detection algorithm for MODIS, Remote Sens. Environ., 87(2–3), 273–282,
893 doi:10.1016/S0034-4257(03)00184-6, 2003.
894 Grythe, H., Kristiansen, N. I., Groot Zwaaftink, C. D., Eckhardt, S., Ström, J., Tunved, P.,
895 Krejci, R. and Stohl, A.: A new aerosol wet removal scheme for the Lagrangian particle
896 model FLEXPARTv10, Geosci. Model Dev., 10, 1447–1466, doi:10.5194/gmd-10-1447-
897 2017, 2017.
898 Hansen, J. and Nazarenko, L.: Soot climate forcing via snow and ice albedos, Proc. Natl.
899 Acad. Sci. U. S. A., 101(2), 423–428, doi:10.1073/pnas.2237157100, 2004.
900 Hansen, J., Sato, M., Ruedy, R., Nazarenko, L., Lacis, A., Schmidt, G. A., Russell, G., Aleinov,
901 I., Bauer, M., Bauer, S., Bell, N., Cairns, B., Canuto, V., Chandler, M., Cheng, Y., Del Genio, A.,
902 Faluvegi, G., Fleming, E., Friend, A., Hall, T., Jackman, C., Kelley, M., Kiang, N., Koch, D.,
903 Lean, J., Lerner, J., Lo, K., Menon, S., Miller, R., Minnis, P., Novakov, T., Oinas, V., Perlwitz,
904 J., Perlwitz, J., Rind, D., Romanou, A., Shindell, D., Stone, P., Sun, S., Tausnev, N., Thresher,
905 D., Wielicki, B., Wong, T., Yao, M. and Zhang, S.: Efficacy of climate forcings, J. Geophys.
906 Res. D Atmos., 110(18), 1–45, doi:10.1029/2005JD005776, 2005.
907 Hao, W. M. and Ward, D. E.: Methane production from global biomass burning, J.
908 Geophys. Res. Atmos., 98(D11), 20657–20661, doi:10.1029/93JD01908, 1993.
909 Hao, W. M., Petkov, A., Nordgren, B. L., Silverstein, R. P., Corley, R. E., Urbanski, S. P.,
910 Evangeliou, N., Balkanski, Y. and Kinder, B.: Daily black carbon emissions from fires in
911 Northern Eurasia from 2002 to 2013, Geosci. Model Dev., 9, 4461–4474,
912 doi:10.5194/gmd-9-4461-2016, 2016.
913 Holben, B. N.: Characteristics of maximum-value composite images from temporal
914 AVHRR data, Int. J. Remote Sens., 7(11), 1417–1434, doi:10.1080/01431168608948945,

915 1986.
916 Holben, B. N., Eck, T. F., Slutsker, I., Tanré, D., Buis, J. P., Setzer, A., Vermote, E., Reagan, J.
917 A., Kaufman, Y. J., Nakajima, T., Lavenu, F., Jankowiak, I. and Smirnov, A.: AERONET—A
918 Federated Instrument Network and Data Archive for Aerosol Characterization, Remote
919 Sens. Environ., 66(1), 1–16, doi:10.1016/S0034-4257(98)00031-5, 1998.
920 Hosseini, S., Li, Q., Cocker, D., Weise, D., Miller, A., Shrivastava, M., Miller, J. W.,
921 Mahalingam, S., Princevac, M. and Jung, H.: Particle size distributions from laboratory-
922 scale biomass fires using fast response instruments, Atmos. Chem. Phys., 10(16), 8065–
923 8076, doi:10.5194/acp-10-8065-2010, 2010.
924 IPCC: Climate Change 2013: The Physical Science Basis. Contribution to the Fifth
925 Assessment Report of the Intergovernmental Panel on Climate Change., edited by T. F.
926 Stocker, D. Qin, G.-K. Plattner, M. M. B. Tignor, S. K. Allen, J. Boschung, A. Nauels, Y. Xia, V.
927 Bex, and P. M. Midgley, Cambridge University Press., 2013.
928 Jedrzejek, B., Drees, B., Daniëls, F. J. A. and Hölzel, N.: Vegetation pattern of mountains in
929 West Greenland - a baseline for long-term surveillance of global warming impacts, Plant
930 Ecol. Divers., 6(3–4), 405–422, doi:10.1080/17550874.2013.802049, 2013.
931 Justice, C. O., Giglio, L., Korontzi, S., Owens, J., Morisette, J. T., Roy, D., Descloitres, J.,
932 Alleaume, S., Petitcolin, F. and Kaufman, Y.: The MODIS fire products, Remote Sens.
933 Environ., 83(1–2), 244–262, doi:10.1016/S0034-4257(02)00076-7, 2002.
934 Kaiser, J. W., Heil, A., Andreae, M. O., Benedetti, A., Chubarova, N., Jones, L., Morcrette, J. J.,
935 Razinger, M., Schultz, M. G., Suttie, M. and Van Der Werf, G. R.: Biomass burning
936 emissions estimated with a global fire assimilation system based on observed fire
937 radiative power, Biogeosciences, 9(1), 527–554, doi:10.5194/bg-9-527-2012, 2012.
938 Kato, S., Ackerman, T. P., Mather, J. H. and Clothiaux, E. E.: The k-distribution method and
939 correlated-k approximation for a shortwave radiative transfer model, J. Quant.
940 Spectrosc. Radiat. Transf., 62(1), 109–121, doi:10.1016/S0022-4073(98)00075-2, 1999.
941 Keegan, K. M., Albert, M. R., Mcconnell, J. R. and Baker, I.: Climate change and forest fires
942 synergistically drive widespread melt events of the Greenland Ice Sheet, , 1–4,
943 doi:10.1073/pnas.1405397111, 2014.
944 Key, C. H. and Benson, N. C.: Landscape assessment: Sampling and analysis methods,
945 USDA For. Serv. Gen. Tech. Rep. RMRS-GTR-164-CD, (June), 1–55,
946 doi:10.1002/app.1994.070541203, 2006.
947 Klimont, Z., Kupiainen, K., Heyes, C., Purohit, P., Cofala, J., Rafaj, P., Borken-Kleefeld, J. and
948 Schöpp, W.: Global anthropogenic emissions of particulate matter including black
949 carbon, Atmos. Chem. Phys., 17, 8681–8723, doi:10.5194/acp-17- 50 8681-2017, 2017.
950 Lavoie, C. and Pellerin, S.: Fires in temperate peatlands (southern Quebec): past and
951 recent trends, Can. J. Bot., 85(3), 263–272, doi:10.1139/B07-012, 2007.
952 Legrand, M., McConnell, J., Fischer, H., Wolff, E. W., Preunkert, S., Arienzo, M., Chellman,
953 N., Leuenberger, D., Maselli, O., Place, P., Sigl, M., Schï¿½pbach, S. and Flannigan, M.:
954 Boreal fire records in Northern Hemisphere ice cores: A review, Clim. Past, 12(10),
955 2033–2059, doi:10.5194/cp-12-2033-2016, 2016.
956 Leino, K., Riuttanen, L., Nieminen, T., Väänänen, R., Pohja, T., Keronen, P., Järvi, L., Aalto,
957 P. P., Virkkula, A., Kerminen, V. M., Petäjä, T., Kulmala, M., Nieminen, T., Dal Maso, M. and
958 Virkkula, A.: Biomass-burning smoke episodes in Finland from eastern European
959 wildfires, Boreal Environ. Res., 19(x), 275–292, 2014.
960 Lelieveld, J., Evans, J. S., Fnais, M., Giannadaki, D. and Pozzer, A.: The contribution of
961 outdoor air pollution sources to premature mortality on a global scale., Nature,
962 525(7569), 367–71, doi:10.1038/nature15371, 2015.
963 Leung, F. Y. T., Logan, J. A., Park, R., Hyer, E., Kasischke, E., Streets, D. and Yurganov, L.:

964   Impacts of enhanced biomass burning in the boreal forests in 1998 on tropospheric
965   chemistry and the sensitivity of model results to the injection height of emissions, J.
966   Geophys. Res. Atmos., 112(10), 1–15, doi:10.1029/2006JD008132, 2007.
967   Long, C. M., Nascarella, M. A. and Valberg, P. A.: Carbon black vs. black carbon and other
968   airborne materials containing elemental carbon: Physical and chemical distinctions,
969   Environ. Pollut., 181, 271–286, doi:10.1016/j.envpol.2013.06.009, 2013.
970   Magnan, G., Lavoie, M. and Payette, S.: Impact of fire on long-term vegetation dynamics
971   of ombrotrophic peatlands in northwestern Québec, Canada, Quat. Res., 77(1), 110–121,
972   doi:http://dx.doi.org/10.1016/j.yqres.2011.10.006, 2012.
973   Massling, A., Nielsen, I. E., Kristensen, D., Christensen, J. H., Sorensen, L. L., Jensen, B.,
974   Nguyen, Q. T., Nøjgaard, J. K., Glasius, M. and Skov, H.: Atmospheric black carbon and
975   sulfate concentrations in Northeast Greenland, Atmos. Chem. Phys., 15(16), 9681–9692,
976   doi:10.5194/acp-15-9681-2015, 2015.
977   Mayer, B. and Kylling, A.: Technical note: The libRadtran software package for radiative
978   transfer calculations - description and examples of use, Atmos. Chem. Phys., 5(7), 1855–
979   1877, doi:10.5194/acp-5-1855-2005, 2005.
980   Myhre, G., Shindell, D., Bréon, F.-M., Collins, W., Fuglestvedt, J., Huang, J., Koch, D.,
981   Lamarque, J.-F., Lee, D., Mendoza, B., Nakajima, T., Robock, A., Stephens, G., Takemura, T.
982   and Zhang, H.: Anthropogenic and Natural Radiative Forcing, in Climate Change 2013:
983   The Physical Science Basis. Contribution of Working Group I to the Fifth Assessment
984   Report of the Intergovernmental Panel on Climate Change, edited by Stocker, T.F., D. Qin,
985   G.-K. Plattner, M. Tignor, S. K. Allen, J. Boschung, A. Nauels, Y. Xia, V. Bex, and P. M.
986   Midgley, pp. 659–740, Cambridge University Press, Cambridge, United Kingdom and
987   New York, NY, USA., 2013.
988   NASA: FIRMS. Web Fire Mapper, [online] Available from:
989   https://firms.modaps.eosdis.nasa.gov/firemap/ (Accessed 5 September 2017a), 2017.
990   NASA: Roundtable: The Greenland Wildfire, [online] Available from:
991   https://earthobservatory.nasa.gov/blogs/earthmatters/2017/08/10/roundtable-the-
992   greenland-wildfire/ (Accessed 6 September 2017b), 2017.
993   NASA: Wildfires Continue to Beleaguer Western Canada, [online] Available from:
994   https://www.nasa.gov/image-feature/goddard/2017/wildfires-continue-to-beleaguer-
995   western-canada (Accessed 29 October 2017c), 2017.
996   New Scientist Magazine: Largest ever wildfire in Greenland seen burning from space,
997   [online] Available from: https://www.newscientist.com/article/2143159-largest-ever-
998   wildfire-in-greenland-seen-burning-from-space/ (Accessed 6 September 2017), 2017.
999   Page, S. E., Siegert, F., Rieley, J. O., Boehm, H.-D. V., Jada, A. and Limin, S.: The amount of
1000   carbon released from peat and forest fires in Indonesia during 1997, Nature, 420(19),
1001   61–65, doi:10.1038/nature01131, 2015.
1002   Paugam, R., Wooster, M. and Atherton, J.: Development and optimization of a wildfire
1003   plume rise model based on remote sensing data inputs – Part 2, , doi:10.5194/acpd-15-
1004   9815-2015, 2015.
1005   Pokhrel, R. P., Wagner, N. L., Langridge, J. M., Lack, D. A., Jayarathne, T., Stone, E. A.,
1006   Stockwell, C. E., Yokelson, R. J. and Murphy, S. M.: Parameterization of single-scattering
1007   albedo (SSA) and absorption Ångström exponent (AAE) with EC/OC for aerosol
1008   emissions from biomass burning, Atmos. Chem. Phys., 16(15), 9549–9561,
1009   doi:10.5194/acp-16-9549-2016, 2016.
1010   Polashenski, C. M., Dibb, J. E., Flanner, M. G., Chen, J. Y., Courville, Z. R., Lai, A. M., Schauer,
1011   J. J., Shafer, M. M. and Bergin, M.: Neither dust nor black carbon causing apparent albedo
1012   decline in Greenland's dry snow zone: Implications for MODIS C5 surface reflectance,

23

1013   Geophys. Res. Lett., 42(21), 9319–9327, doi:10.1002/2015GL065912, 2015.

1014   Randerson, J. T., Chen, Y., Van Der Werf, G. R., Rogers, B. M. and Morton, D. C.: Global
1015   burned area and biomass burning emissions from small fires, J. Geophys. Res.
1016   Biogeosciences, 117(4), doi:10.1029/2012JG002128, 2012.

1017   Reddy, A. D., Hawbaker, T. J., Wurster, F., Zhu, Z., Ward, S., Newcomb, D. and Murray, R.:
1018   Quantifying soil carbon loss and uncertainty from a peatland wildfire using multi-
1019   temporal LiDAR, Remote Sens. Environ., 170, 306–316, doi:10.1016/j.rse.2015.09.017,
1020   2015.

1021   Rémy, S., Veira, A., Paugam, R., Sofiev, M., Kaiser, J. W., Marenco, F., Burton, S. P.,
1022   Benedetti, A., Engelen, R. J., Ferrare, R. and Hair, J. W.: Two global data sets of daily fire
1023   emission injection heights since 2003, , 2921–2942, doi:10.5194/acp-17-2921-2017,
1024   2017.

1025   Restuccia, F., Ptak, N. and Rein, G.: Self-heating behavior and ignition of shale rock,
1026   Combust. Flame, 176, 213–219, doi:10.1016/j.combustflame.2016.09.025, 2017a.

1027   Restuccia, F., Huang, X. and Rein, G.: Self-ignition of natural fuels: Can wildfires of
1028   carbon-rich soil start by self-heating?, Fire Saf. J., 91(February), 828–834,
1029   doi:10.1016/j.firesaf.2017.03.052, 2017b.

1030   Sand, M., Berntsen, T. K., von Salzen, K., Flanner, M. G., Langner, J. and Victor, D. G.:
1031   Response of Arctic temperature to changes in emissions of short-lived climate forcers,
1032   Nat. Clim. Chang., 6(November), 1–5, doi:10.1038/nclimate2880, 2015.

1033   von Schneidemesser, E., Schauer, J. J., Hagler, G. S. W. and Bergin, M. H.: Concentrations
1034   and sources of carbonaceous aerosol in the atmosphere of Summit, Greenland, Atmos.
1035   Environ., 43(27), 4155–4162, doi:10.1016/j.atmosenv.2009.05.043, 2009.

1036   Seiler, W. and Crutzen, P. J.: Estimates of gross and net fluxes of carbon between the
1037   biosphere and the atmosphere from biomass burning, Clim. Change, 2(3), 207–247,
1038   doi:10.1007/BF00137988, 1980.

1039   SERMITSIAQ: Se billeder: Naturbrand udvikler kraftig røg, , in Danish [online] Available
1040   from: http://sermitsiaq.ag/se-billeder-naturbrand-udvikler-kraftig-roeg (Accessed 6
1041   September 2017), 2017.

1042   Shetler, G., Turetsky, M. R., Kane, E. and Kasischke, E.: Sphagnum mosses limit total
1043   carbon consumption during fire in Alaskan black spruce forests, Can. J. For. Res., 38(8),
1044   2328–2336, doi:10.1139/X08-057, 2008.

1045   Shi, Y., Matsunaga, T., Saito, M., Yamaguchi, Y. and Chen, X.: Comparison of global
1046   inventories of CO2 emissions from biomass burning during 2002-2011 derived from
1047   multiple satellite products, Environ. Pollut., 206, 479–487,
1048   doi:10.1016/j.envpol.2015.08.009, 2015.

1049   Skeie, R. B., Berntsen, T., Myhre, G., Pedersen, C. A., Strãm, J., Gerland, S. and Ogren, J. A.:
1050   Black carbon in the atmosphere and snow, from pre-industrial times until present,
1051   Atmos. Chem. Phys., 11(14), 6809–6836, doi:10.5194/acp-11-6809-2011, 2011.

1052   Smirnov, N. S., Korotkov, V. N. and Romanovskaya, A. A.: Black carbon emissions from
1053   wildfires on forest lands of the Russian Federation in 2007–2012, Russ. Meteorol.
1054   Hydrol., 40(7), 435–442, doi:10.3103/S1068373915070018, 2015.

1055   Stamnes, K., Tsay, S.-C., Wiscombe, W. and Jayaweera, K.: Numerically stable algorithm
1056   for discrete-ordinate-method radiative transfer in multiple scattering and emitting
1057   layered media, Appl. Opt., 27(12), 2502, doi:10.1364/AO.27.002502, 1988.

1058   Stendel, M., Christensen, J. H. and Petersen, D.: Arctic Climate and Climate Change with a
1059   Focus on Greenland, Adv. Ecol. Res., 40(07), 13–43, doi:10.1016/S0065-
1060   2504(07)00002-5, 2008.

1061   Stockwell, C. E., Jayarathne, T., Cochrane, M. A., Ryan, K. C., Putra, E. I., Saharjo, B. H.,

24

1062 Nurhayati, A. D., Albar, I., Blake, D. R., Simpson, I. J., Stone, E. A. and Yokelson, R. J.: Field
1063 measurements of trace gases and aerosols emitted by peat fires in Central Kalimantan,
1064 Indonesia, during the 2015 El Niño, Atmos. Chem. Phys., 16(18), 11711–11732,
1065 doi:10.5194/acp-16-11711-2016, 2016.
1066 Stohl, A., Forster, C., Frank, A., Seibert, P. and Wotawa, G.: Technical note: The Lagrangian
1067 particle dispersion model FLEXPART version 6.2, Atmos. Chem. Phys., 5(9), 2461–2474,
1068 doi:10.5194/acp-5-2461-2005, 2005.
1069 Stohl, A., Andrews, E., Burkhart, J. F., Forster, C., Herber, A., Hoch, S. W., Kowal, D.,
1070 Lunder, C., Mefford, T., Ogren, J. A., Sharma, S., Spichtinger, N., Stebel, K., Stone, R., Ström,
1071 J., Tørseth, K., Wehrli, C. and Yttri, K. E.: Pan-Arctic enhancements of light absorbing
1072 aerosol concentrations due to North American boreal forest fires during summer 2004, J.
1073 Geophys. Res. Atmos., 111(22), 1–20, doi:10.1029/2006JD007216, 2006.
1074 Stohl, A., Berg, T., Burkhart, J. F., Fjǽraa, A. M., Forster, C., Herber, A., Hov, Ø., Lunder, C.,
1075 McMillan, W. W., Oltmans, S., Shiobara, M., Simpson, D., Solberg, S., Stebel, K., Ström, J.,
1076 Tørseth, K., Treffeisen, R., Virkkunen, K. and Yttri, K. E.: Arctic smoke – record
1077 high air pollution levels in the European Arctic due to agricultural fires in Eastern
1078 Europe in spring 2006, Atmos. Chem. Phys., 7(2), 511–534, doi:10.5194/acp-7-511-
1079 2007, 2007.
1080 Stohl, A., Prata, A. J., Eckhardt, S., Clarisse, L., Durant, A., Henne, S., Kristiansen, N. I.,
1081 Minikin, A., Schumann, U., Seibert, P., Stebel, K., Thomas, H. E., Thorsteinsson, T., Tørseth,
1082 K. and Weinzierl, B.: Determination of time-and height-resolved volcanic ash emissions
1083 and their use for quantitative ash dispersion modeling: The 2010 Eyjafjallajokull
1084 eruption, Atmos. Chem. Phys., 11(9), 4333–4351, doi:10.5194/acp-11-4333-2011, 2011.
1085 Stohl, A., Klimont, Z., Eckhardt, S., Kupiainen, K., Shevchenko, V. P., Kopeikin, V. M. and
1086 Novigatsky, A. N.: Black carbon in the Arctic: The underestimated role of gas flaring and
1087 residential combustion emissions, Atmos. Chem. Phys., 13(17), 8833–8855,
1088 doi:10.5194/acp-13-8833-2013, 2013.
1089 Stroeve, J., Box, J. E., Gao, F., Liang, S., Nolin, A. and Schaaf, C.: Accuracy assessment of the
1090 MODIS 16-day albedo product for snow: Comparisons with Greenland in situ
1091 measurements, Remote Sens. Environ., 94(1), 46–60, doi:10.1016/j.rse.2004.09.001,
1092 2005.
1093 Sunderman, S. O. and Weisberg, P. J.: Remote sensing approaches for reconstructing fire
1094 perimeters and burn severity mosaics in desert spring ecosystems, Remote Sens.
1095 Environ., 115(9), 2384–2389, doi:10.1016/j.rse.2011.05.001, 2011.
1096 Turetsky, M. R., Donahue, W. F. and Benscoter, B. W.: Experimental drying intensifies
1097 burning and carbon losses in a northern peatland, Nat. Commun., 2, 514,
1098 doi:10.1038/ncomms1523, 2011.
1099 Turetsky, M. R., Benscoter, B., Page, S., Rein, G., van der Werf, G. R. and Watts, A.: Global
1100 vulnerability of peatlands to fire and carbon loss, Nat. Geosci., 8(1), 11–14,
1101 doi:10.1038/ngeo2325, 2014.
1102 Urbanski, S. P., Hao, W. M. and Nordgren, B.: The wildland fire emission inventory:
1103 Western United States emission estimates and an evaluation of uncertainty, Atmos.
1104 Chem. Phys., 11(24), 12973–13000, doi:10.5194/acp-11-12973-2011, 2011.
1105 Wandji Nyamsi, W., Arola, A., Blanc, P., Lindfors, a. V., Cesnulyte, V., Pitkänen, M. R. a. and
1106 Wald, L.: Technical Note: A novel parameterization of the transmissivity due to ozone
1107 absorption in the distribution method and correlated approximation of Kato et al.
1108 (1999) over the UV band, Atmos. Chem. Phys., 15(13), 7449–7456, doi:10.5194/acp-15-
1109 7449-2015, 2015.
1110 Warren, S. G.: Can black carbon in snow be detected by remote sensing?, J. Geophys. Res.

1111   Atmos., 118(2), 779–786, doi:10.1029/2012JD018476, 2013.

1112   Wieder, R. K., Scott, K. D., Kamminga, K., Vile, M. A., Vitt, D. H., Bone, T., Xu, B., Benscoter,
1113   B. W. and Bhatti, J. S.: Postfire carbon balance in boreal bogs of Alberta, Canada, Glob.
1114   Chang. Biol., 15(1), 63–81, doi:10.1111/j.1365-2486.2008.01756.x, 2009.

1115   Winiger, P., Andersson, A., Eckhardt, S., Stohl, A., Semiletov, I. P., Dudarev, O. V., Charkin,
1116   A., Shakhova, N., Klimont, Z., Heyes, C. and Gustafsson, Ö.: Siberian Arctic black carbon
1117   sources constrained by model and observation, Proc. Natl. Acad. Sci., 114(7), E1054–
1118   E1061, doi:10.1073/pnas.1613401114, 2017.

1119   Winker, D. M., Vaughan, M. A., Omar, A., Hu, Y., Powell, K. A., Liu, Z., Hunt, W. H. and
1120   Young, S. A.: Overview of the CALIPSO mission and CALIOP data processing algorithms, J.
1121   Atmos. Ocean. Technol., 26(11), 2310–2323, doi:10.1175/2009JTECHA1281.1, 2009.

1122   Wu, D., Huang, X., Norman, F., Verplaetsen, F., Berghmans, J. and Van Den Bulck, E.:
1123   Experimental investigation on the self-ignition behaviour of coal dust accumulations in
1124   oxy-fuel combustion system, Fuel, 160, 245–254, doi:10.1016/j.fuel.2015.07.050, 2015.

1125   Zhuravleva, T. B., Kabanov, D. M., Nasrtdinov, I. M., Russkova, T. V., Sakerin, S. M.,
1126   Smirnov, A. and Holben, B. N.: Radiative characteristics of aerosol during extreme fire
1127   event over Siberia in summer 2012, Atmos. Meas. Tech., 10(1), 179–198,
1128   doi:10.5194/amt-10-179-2017, 2017.

1129
1130

FIGURE LEGENDS
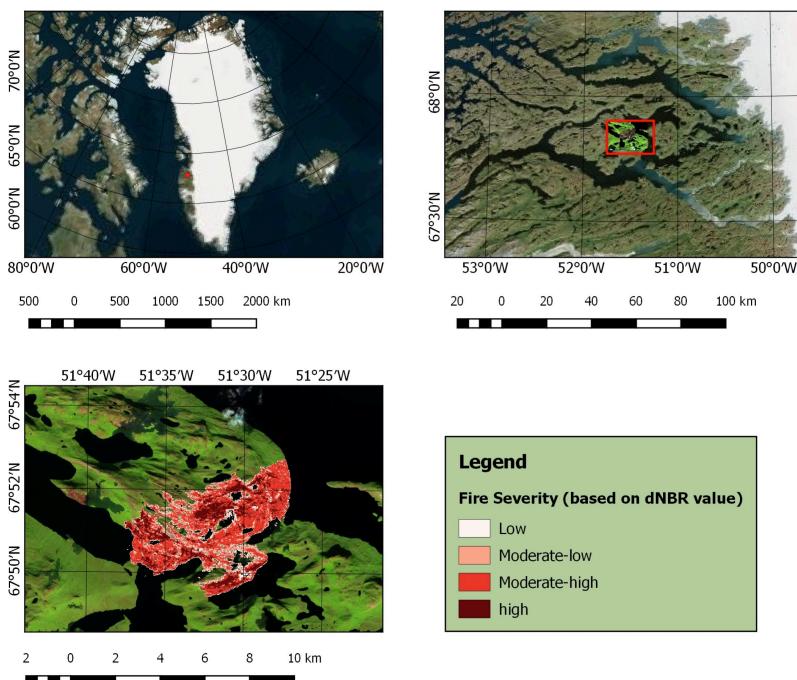
1132
1133 **Figure 1.** Map of Greenland (upper left) and zoomed map marked with fire location (upper
1134 right and burned area classification (bottom) in terms of fire severity according to Sentinel 2A
1135 images for fires burning in Greenland in August 2017. To delineate fire perimeters, both
1136 Landsat 8 OLI and Sentinel 1A – 2A data were used (**Table 1**).

1137

Nikolaos Evangeliou 21/6/2018 20:09
Deleted: Table 1

(a) Vertical distribution
of BC concentrations over time
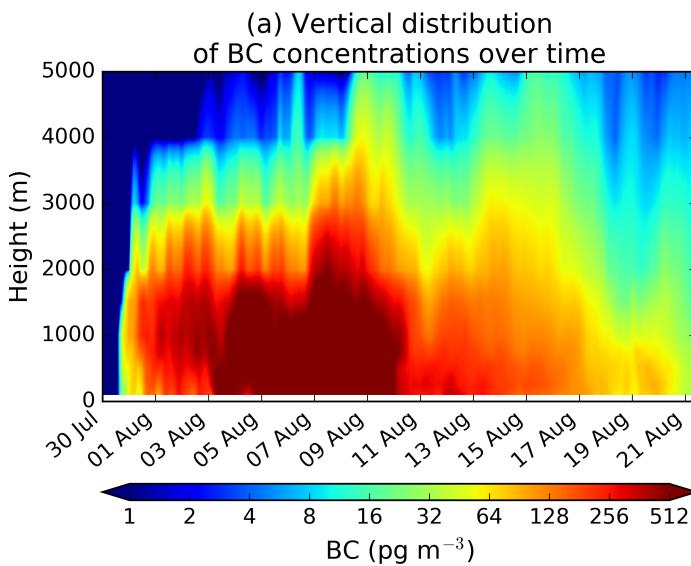
(b) Deposition of BC from Greenland fires
(31 August 2017)
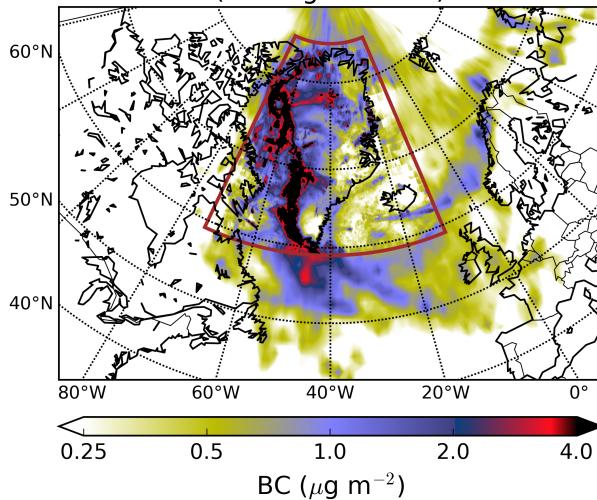
Figure 2. (a) Time-series of vertical distribution of BC concentrations averaged over the area of Greenland in summer 2017 as a function of time. (b) Total (wet and dry) deposition of BC (in μg m^{-2}) from Greenland fires until 31 August 2017. The colored rectangle depicts the nested high-resolution domain.

Nikolaos Evangeliou 8/6/2018 10:33
Deleted: Vertical

Nikolaos Evangeliou 8/6/2018 10:34
Deleted: from the fires in

Nikolaos Evangeliou 8/6/2018 10:38
Deleted: n

1148

(a) Snow concentrations of BC
based on snow accumulation from ECMWF

(b) Dry to total deposition ratio
from the Greenland fires

BC (ng g^{-1})

Dry/(Wet+Dry)

1149
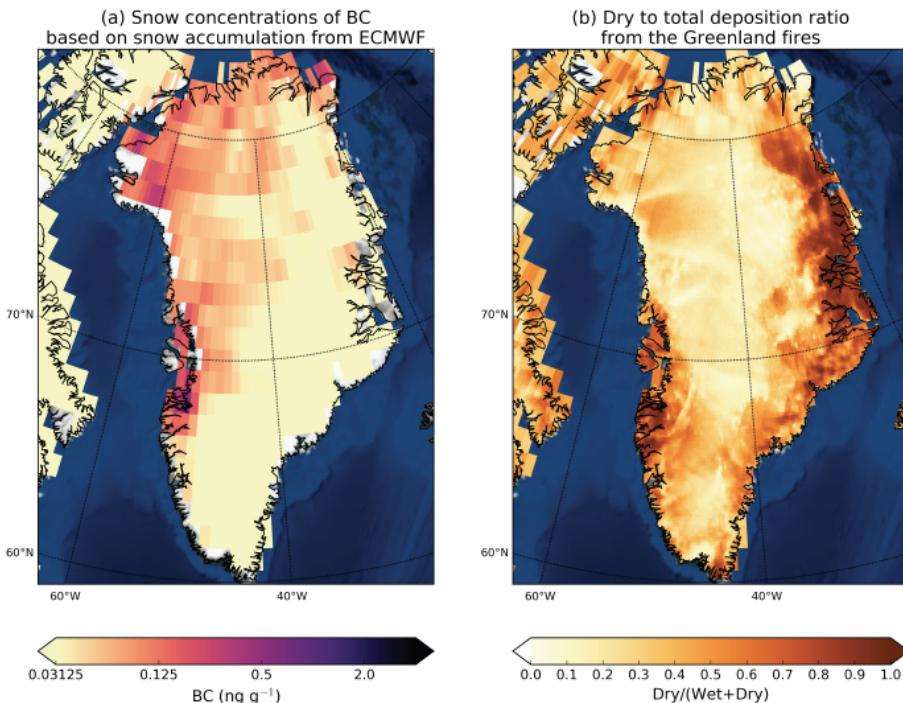
Figure 3. (a) Calculated snow concentrations of BC over Greenland based on the modeled deposition and the snow precipitation (large scale and convective) in the operational ECMWF data that were used in our simulation (see section 2.3). (b) Dry to total deposition ratio of BC from the 2017 peat fires over Greenland.

1150
1151
1152
1153
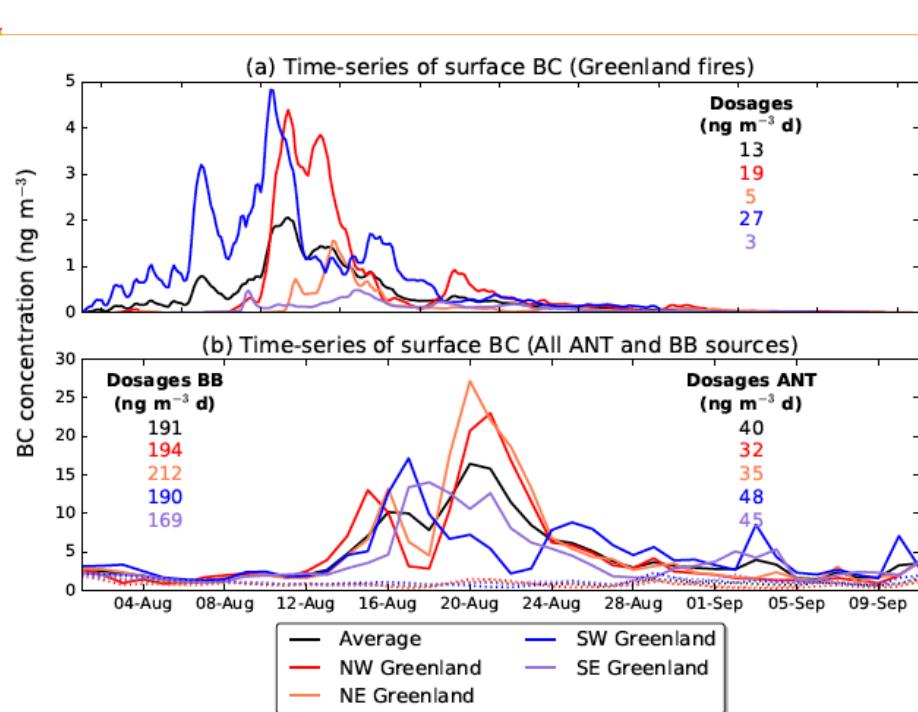
1154

29

1155
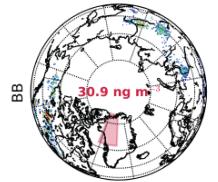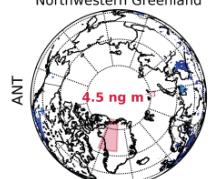
1156

1157 **Figure 4.** (a) Time-series of surface BC concentrations in Northwestern, Northeastern,
1158 Southwestern and Southeastern Greenland from the summer 2017 fires in Western Greenland.
1159 (b) Time-series of surface BC concentrations in Northwestern, Northeastern, Southwestern
1160 and Southeastern Greenland from global anthropogenic (ANT, dashed lines) and biomass
1161 burning (BB, solid lines) emissions for the same period. The numbers represent the respective
1162 dosages (time-integrated concentrations) for the time period shown. The color codes are
1163 reported in the legend.

1164

Figure 5. Contour plot of the vertical distribution of simulated BC (altitude a.g.l. shown on left y-axis) as a function of time (x-axis) and time-series of column-integrated simulated BC (extended right axis) from fires burning outside Greenland (black line) and Greenland fires (cyan stacked area). Column-integrated BC from anthropogenic sources was extremely small and it is not plotted here. Time-series for fine mode (blue) and coarse (red) AOD at 500 nm and total AOD at 400 nm (black) correspond to the right y-axis. The three panels show results for stations (a) Kangerlussuaq, (b) Narsarsuaq and (c) Thule (sorted from the closest to the farthest station).
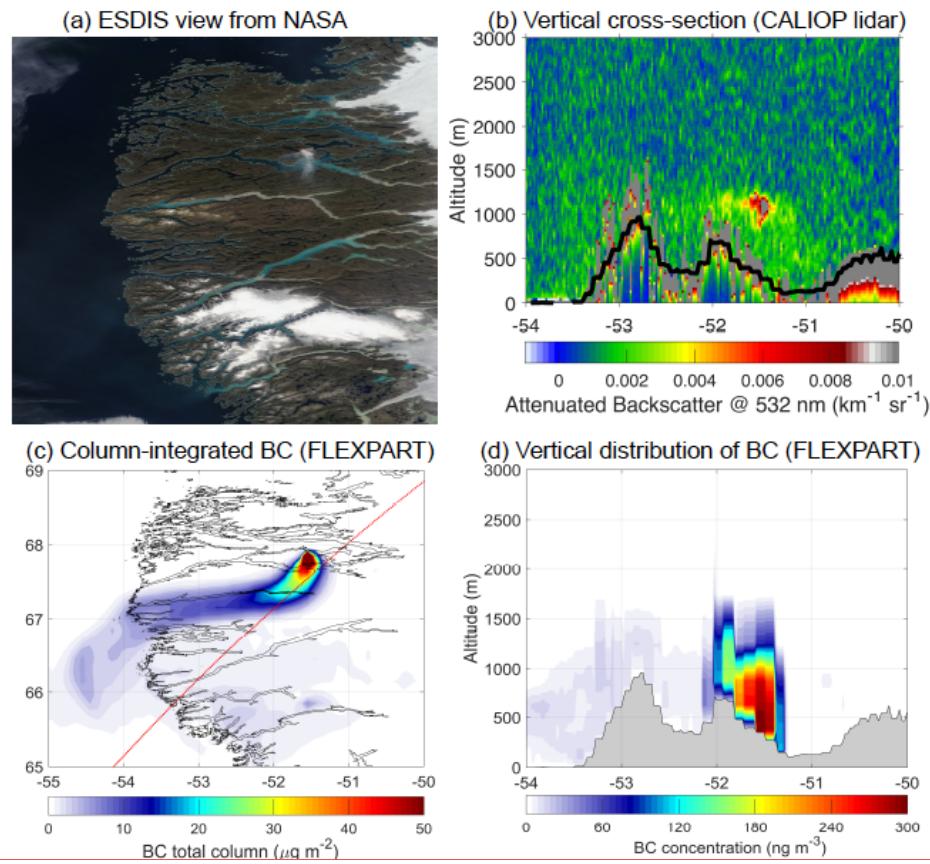
31

Figure 6. (a) Worldview application from the NASA/Goddard Space Flight Center Earth Science Data and Information System (ESDIS) project on 14 August 2017. (b) Vertical cross-section along satellite's route (red line in c) of total attenuated backscatter at a wavelength of 532 nm obtained from the CALIOP lidar on 14 August 2017 at 6 UTC (black line denotes the orography of the area). (c) Column-integrated BC concentration simulated with FLEXPART (read line shows the path of the satellite). (d) Vertical distribution of BC concentrations with longitude as seen with FLEXPART (grey area denotes the orography of the area).
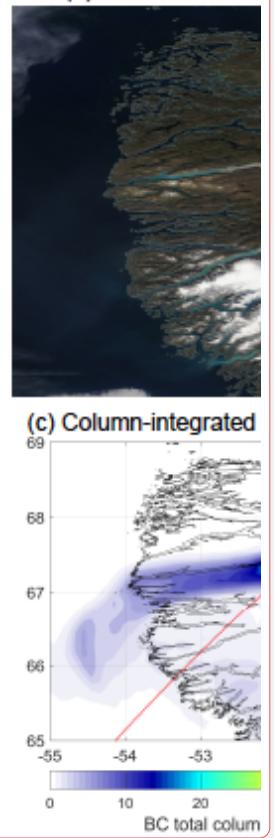
(d) Variation of TOA IRF over Greenland in August 2017
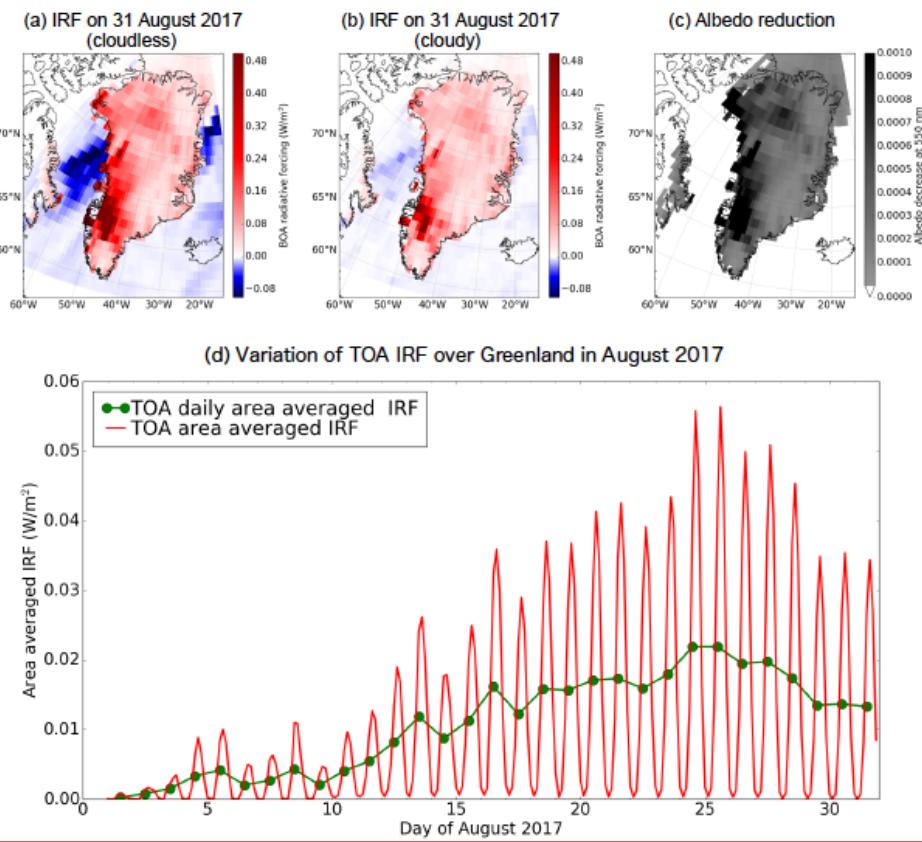
Figure 7. (a) The instantaneous direct BOA RF due to BC from the Greenland fires for cloudless and (b) cloudy conditions on 31 August, and (c) snow albedo reduction due to the total BC deposited as a result of the Greenland fires. (d) Temporal variation of the cloudy TOA IRF over Greenland in August 2017.

Nikolaos Evangeliou 8/6/2018 11:23
Deleted: the

SUPPLEMENTARY FIGURE LEGENDS

Figure S 1. Annual number of active fires over Greenland during the last 17 years as seen from NASA's MODIS satellite (product MSC14DL).

Figure S 2. Fire dynamics in Greenland for the August 2017 fires according to MODIS (magenta dots show active fire hot spots from the MODIS MCD14DL product). Locations of stations with AOD measurements from AERONET are also shown.

Figure S 3. Median injection heights (km above sea level – ASL; left panel) and distribution of longitudinally integrated burned biomass (Tg) as a function of injection altitude (right panel) calculated by PRMv2 for the period between 31 July and 21 August 2017.

Figure S 4. Relative standard deviation of BC deposition for different assumed size distributions of BC normalized against the results for our reference size distribution with a logarithmic mean diameter of 0.25 µm. Particle size distributions with aerodynamic mean diameters of 0.1, 0.25, 0.5, 1, 2, 4, 8 µm and a logarithmic standard deviation of 0.3 were simulated.

Figure S 5. Footprint emissions sensitivities for Northwestern, Northeastern, Southwestern and Southeastern Greenland for the period 31 July to 31 August 2017. Active fires from NASA's MODIS MCD14DL product are shown with red dots.

Figure S 6. Average contribution of biomass burning (upper panels) and anthropogenic emissions (lower panels) to surface concentrations of BC in Northwestern, Northeastern, Southwestern and Southeastern Greenland (in ng m^{-3} per grid cell). Numbers (in red) represent total concentrations in the studied domain, obtained by spatial integration over all source grid cells. Receptor areas in Greenland are highlighted by pink boxes.

Figure S 7. (a) The single scattering albedo (SSA) of BC as a function of wavelength for various modified combustion efficiencies (MCE). The star and dot marked lines are from the parameterization of Pokhrel et al. (2016). (b) The IRF as a function of BC deposited on the

34

1264 Ice Sheet. The calculations were made for cloudless conditions with a snow-covered surface
1265 for noon on 31 August 2017 at 65°N.

Table 1. Start and end date of releases, source of data, type of sensor, burned area and daily increment of burned area, fuel consumption and calculated BC emissions from Eq. 1 during the Greenland fires in 2017. Total numbers for burned area, fuel consumption and BC emissions are highlighted in bold.

Start	End	Source of RS data	Type of sensor	Burned area (ha)	Increment of burned area (ha)	Fuel consumption (t C)	BC emission (kg)
31/07/17	02/08/17	Sentinel 2A	MSI	304	304	15176	3035
02/08/17	03/08/17	Landsat 8 OLI	MSI	428	125	6247	1249
03/08/17	04/08/17	Sentinel 1A	SAR	588	160	7980	1596
04/08/17	05/08/17	Sentinel 1A	SAR	740	152	7621	1524
05/08/17	07/08/17	Sentinel 2A	MSI	1100	359	17966	3593
07/08/17	08/08/17	Sentinel 2A	MSI	1314	214	10706	2141
08/08/17	12/08/17	Landsat 8 OLI	MSI	1868	554	27714	5543
12/08/17	14/08/17	Sentinel 1A	SAR	2005	136	6817	1363
14/08/17	15/08/17	Sentinel 1A	SAR	2169	165	8244	1649
15/08/17	16/08/17	Sentinel 1A	SAR	2209	40	1998	400
16/08/17	19/08/17	Sentinel 1A	SAR	2254	44	2213	443
19/08/17	21/08/17	Sentinel 2A	MSI	2345	92	4579	916
TOTAL					**2345**	**117259**	**23452**

RS - Remote Sensing
MSI - Multispectral Images
SAR - Synthetic Aperture RADAR

RF was calculated at the top and bottom of the atmosphere at 1°×1° resolution.

The IRF includes both the effects of atmospheric BC and BC deposited on the snow. The latter dominates the IRF contributing between 85 to 99 % to the IRF depending on BC amount. Note that the IRF does not include any semi-direct nor indirect effects. Cloudless conditions were assumed in Figure 7a, while in Figure 7b water and ice water clouds were adopted from ECMWF.